X-644-70-110
PREPRINT

NASA TM X- 63938

CARTOGRAPHIC APPLICATIONS OF ORBITAL PHOTOGRAPHY

RONALD G. DALRYMPLE

MARCH 1970

GSFC
GODDARD SPACE FLIGHT CENTER
GREENBELT, MARYLAND

X-644-70-110

CARTOGRAPHIC APPLICATIONS OF ORBITAL PHOTOGRAPHY

Ronald G. Dalrymple
Planetology Branch

March 1970

GODDARD SPACE FLIGHT CENTER
Greenbelt, Maryland

CARTOGRAPHIC APPLICATIONS OF ORBITAL PHOTOGRAPHY

INTRODUCTION

Since the inception of synoptic photography on unmanned, suborbital Viking flights, investigators have developed increasing scientific and technical applications for the photographs. Geologists, meteorologists and oceanographers alike have expanded and supplemented their studies with the areal coverage of the earth obtained on the Synoptic Terrain Photography (S-005) Experiment and the Synoptic Weather Photography (S-006) Experiment. For example, geologists have used the photos for the study and mapping of regional geology on a world-wide scale, and the synoptic view is proving specifically applicable in the study of regional tectonics and geologic education.

The focus of this paper is upon another use made of the experimental photography: the up-dating and revision of contemporary topographic maps. With the large area included per photo (typically 4900 square miles from a spacecraft altitude of 100 miles), the speed of coverage possible, the enhanced detail available from steroscopic viewing, and the absence of such artificial barriers as national boundaries, cartographers now have the opportunity to produce reliable, global maps having a wide range of scales. This synoptic photography can greatly facilitate the work of the field surveyor and supplement available larger scale aircraft photography.

The parallel desirability of both increasing present earth orbital photograhic coverage and of beginning a more permanent orbital photography program is well demonstrated by the unreliable state of numerous contemporary topographic maps. Gemini and Apollo photos, though limited to approximately 34°N and 34°S latitudes, have unveiled sizable cartographic errors and inconsistencies. Such errors are generally the result of incorrect or incomplete topographic mapping based on either inadequate ground or aerial data, or are functions of post-mapping topographic changes. The purpose of this paper is to show a few of the more obvious of these examples, and to illustrate the value of orbital photography in map revision.

Examples are separated into three distinct but related categories: post-mapping changes (the most important), errors of portrayal, and errors of omission. This classification emphasizes the varied discrepancies encountered when comparing or, perhaps more appropriately, contrasting, photograph to map. Examples within each division will be presented in a west to east progression, simulating the direction of flight of manned earth orbital spacecraft. The principal set of maps to be employed in this work are the AMS 1:1,000,000 Series 1301, which are the most reliable maps with a workable scale for this type of study.

POST-MAPPING CHANGES

The first, largest, and most important category to be considered is that of post-mapping changes or, in effect, map obsolescence. The study of post-mapping changes, especially when caused by geologic events, and the subsequent revision and updating of maps from space photography offer an important scientific use of orbital photographs of earth.

The first example in this category is a comparison of two Gemini photographs of the Laguna Ojo de Libre in Baja California. Encountered here is a seemingly anomalous situation concerning lagoon water depths and the corresponding appearance of the lagoon floor. The first of the two photographs was taken from Gemini V on August 21, 1965 at 13:15 PST. It appears to show a lesser water depth, from the greater floor visibility, than the second photograph, taken from Gemini VII on December 8, 1965 at 13:46 PST (Figure 1). The United States Coast and Geodetic Survey tide data, however, indicate a 2.8 foot greater water depth at the time of the Gemini V shot. The anomaly is strengthened by the fact that the Gemini V photo is a low oblique photograph and the Gemini VII a near vertical (the photos have equivalent sun angles, since they were taken at comparable times of the day).

Three possible explanations are offered to explain this apparently contradicting information. The first solution is to simply assume incorrect tide data; it is difficult to accurately compute exact tides for any given time and place of occurrence, especially in remote areas. Numerous variables complicate the computation process, the most important of which is the effect of air pressure and winds in raising or lowering the local water level. Both affect the level in direct proportion to their force and duration, and can create up to 3 or 4 foot tidal differences. Such factors occurring on one or both of the days in question may have produced the anomaly.

An alternative explanation is that geologic or physical changes significant enough to be observed from space occurred within the time span between the taking of the two photographs. Sedimentation may have partly filled the lagoon, but this explanation is improbable. Barring the event of large storms, sedimentary deposits form far too slowly to account for any sizable bottom differences. For example, sedimentation rates of the latitudinally equivalent Texan bays on the Gulf of Mexico range from 0.4 to 1.6 feet per 100 years (Rusnak, 1960).

Since sedimentation per se seems highly improbable as an explanation for the discrepancy, the occurrence of a storm remains as the final possibility. Summer rains, particularly near the coast and highlands, often come in the form of tremendous downpours, sending temporary torrents running down otherwise dry washes and carrying unusual amounts of sediments and plant debris

(Jaeger, 1957). The salty, flat areas surrounding the lagoon are especially susceptible to such inundation. The absence of any significant living streams in the entire Vizcaino-Magdalena area (ibid) support the plausibility of a storm as the cause of a fluctuating water depth in the lagoon. Regardless of the correct solution to this problem, the value of repetitive coverage such as that provided by orbital photography is well illustrated.

The second example to be considered, in Oaxaca state, southern Mexico, is a triangular, deep-blue lake that marks the junction of Rio Tehuantepec and Rio Tequisistlan. This is the reservoir created by the President Benito Juarez Dam, and provides an excellent example of man-made topographic changes observable from space. The dam was constructed between 1956 and 1961, and has made AMS 1:1,000,000 map NE15, which does not show the reservoir (Figure 2), at least partially obsolete. The map is based on 1954 data.

Another example is seen to the southeast in Honduras-Nicaragua, where we find three major areas of discrepancy between a Gemini V photograph and AMS 1:1,000,000 map ND 16. The first error is a stream meander along the Coco River, near the town of Bilas. The river has four adjacent meander loops in it, as shown by the photograph, but the map portrays a straighter course (Figure 3). Forty-five miles north, the second area of discrepancy is apparent about Islas Tonsin, which lies within Laguna Caratasca. The photograph shows that the area contains lagoonal and coastal structures similar in appearance to those of Laguna Madre, Mexico, and Cape Hatteras, N. C., with a continuity of land mass evident. The map, however, portrays twelve distinct islands within the lake, and the southern shoreline of the lake is incorrectly shown. The third discrepancy is seen with Rio Patuca, west of Laguna Caratasca. Here, as with the Coco River, stream meanders are differently shown on photograph and map. As in the Juarez reservoir example, the cause of these errors probably lies in map data obsolescence; map data is from 1937.

Other orbital photographs show the elliptical Lago de Poopo in Bolivia, 19° south of the equator. Comparing this frame to the AMS 1:1,000,000 map of the area, SE-19, it is recognized that the boundary of the lake is incorrect in several places, although its basic form is fairly accurate on the map (Figure 4). The surrounding area is described as marsh in the legend, presumably accounting for the shoreline errors. The lake is fed by the curling Rio Desaguadero, and it is here that the first of two more significant discrepancies is found. A sizable lake, eleven miles in its greatest dimension, straddles the river west of the town of Machacamarca, as shown on a GT-5 photograph, but not on an Apollo 9 photograph. The AMS maps fail to illustrate any such lake, but denote the area as marsh. Climatic changes such as these may be studied to advantage from space. Reference to another photograph, taken from Gemini IX, reveals the second major discrepancy found in the same general area (Figure 46). Here,

the map portrays Lago de Coipasa, 17 miles in length, at 55 miles west of the southern tip of Lago de Poopo, but the photo shows only four small water bodies at this location; no continuous large lake as that portrayed on the map exists. The map was reprinted in 1952 from an AGS map dated 1922.

On the northeast coast of Brazil, the broad mouth of the Amazon River offers an excellent example of fluvial sedimentation; fluctuating currents constantly change the configuration of the low-lying islands at the river mouth. On comparing the depositional features as they appear on a Gemini VII photograph to AMC Hydrographic Chart L-28, 1:1,000,000 scale, four major areas of discordance can be readily identified (Figure 5). All of these cartographic discrepancies concern erosional modifications of the area over a relatively short period of time; the synoptic photograph was taken in December, 1965, and the latest air photos on which the map is based had been taken only 9 months earlier. The value of orbital photography in correcting such rapid map obsolescence, as well as its value in the fields of oceanography and marine geology, is apparent.

Another region influenced by rapid major hydrographic fluctuations is found near the Niger River in Mali, North Africa. Numerous of the fresh and salt water lakes near Tombouctou, shown on a Gemini VI shot, differ in size and shape from their map plots on AMS 1:1,000,000 ND, NE 30, compiled in 1956 and 1942, respectively (Figure 6). Much of the area, particularly adjacent to the river bed, is described in the legend to be subject to seasonal inundation, and this stands as the probable explanation for the recognized differences.

A larger and perhaps more interesting African lacustrine feature is Lake Chad, bordered by the countries of Chad, Niger, Nigeria, and Cameroon. Although fed by the Chari River, this pear-shaped, fresh-water lake is slowly diminishing in size by intense evaporation, and averages only 3 to 4 feet in depth. The resultant potential for map errors created by these factors is manifest when comparing a Gemini IX photograph of the feature with AMS 1:1,000,000 map ND 33, published as recently as 1956 (Figure 7). The map portrays Lake Chad as narrower and smaller than is indicated on the photograph, particularly at the bottleneck near the middle. As with previous examples, the shores of the lake are described as marsh. A second discrepancy is found at the Dillia Sebkha, a salt playa northwest of Lake Chad, with the map portraying a longer and larger playa than does the photo. Such playas, consisting of sun-baked clay, silt and salt, are formed in desert areas by the evaporation of temporary lakes, formed in turn by sporadic rainfalls and internal drainage. Over a period of years, alternate filling and drying could well account for the discrepancies seen here between the photograph and map.

Far to the southeast, in Ethiopia, two lakes below Addis Ababa have been omitted from AMS 1:1,000,000 maps NB, NC 37. A Gemini IV near vertical

photograph of this area shows the first lake to be approximately three miles east of Lake Auasa, and the second twenty miles northeast of Lake Zuai near the cities of Gorobuta and Coca (Figure 8). Both lakes cover an area of about 40 square miles in regions that are denoted as permanent swamp. Significant changes in water level seem to be the explanation for these discrepancies, an hypothesis further supported by Lake Langanno, which appears on the photo to be shallower than its neighbor lakes. A final use can be made of this photograph, concerning another field of study, meteorology. The lakes occupy a region surrounded by scattered cumulus clouds, but few of these are seen directly over or immediately near the lakes. This might indicate to a meteorologist that connective buildup occurs more slowly over the lake than over the adjacent land areas.

Bordering on Kashmir, India, Nepal and China, the Tibetan Plateau provides several notable examples of map obsolescence. Despite obscuring clouds, a low-oblique Gemini V photo shows that a large portion of Charol Tsho, an intermittent salt lake, does not appear on AMS 1:1,000,000 map NI-44, compiled in 1950 (Figure 9). Nearby Heze Tsho, Horpa Tsho, and Traggon Tsho are easily distinguishable on the map, but differ significantly in shape from those on the more recent photograph (August, 1965). In fact, it is difficult to successfully correlate photograph to map for the entire area.

A more striking example of the same type of map discrepancy is seen 190 miles to the southeast with a Gemini V photo covering Nganglaring Tso, Tabia Tsaka, Shovo Tzo, Turok Tso and Poru Tso. Comparison of the shot with AMS 1:1,000,000 maps NH-44, 45 shows that Nganglaring Tso is the most accurately plotted, although its shoreline is not precise and the small island in it is incorrectly delineated (Figure 10). Additional errors are seen with Tabia Tsaka, which is illustrated as a fresh water lake with poorly defined limits, but is indicated by the photograph to actually be two adjacent lakes of approximately equal size. The northern lake is brownish in hue and probably shallow, whereas the southern is a salt playa. Shovo Tso appears to be almost twice as large as it has been mapped. Tarok Tso, like Tabia Tsaka, is described as a poorly defined fresh water lake, and it occupies a region covering about 35 square miles. The photograph, however, reveals it to be much larger than shown on the map, covering about 320 square miles. This discrepancy in area is almost one order of magnitude.

It is instructive to note here that a recent Apollo 7 photograph (October, 1968), taken of approximately the same area as the previous Gemini shot (August, 1965), indicates an apparent increased water depth, recognized by deeper hues of blue, within Nganglaring Tsho on the more recent photo. Several tiny islands within the dagger-shaped lake seen on the Gemini photo are not visible on that from Apollo.

As a final representative of dynamic geologic features, let us consider the mouth of the Yanztse River, near Shang-hai, China. Influenced by strong currents similar to those of the Amazon River, Ch'ung-ming Tao and other nearby islands within the river mouth are constantly changing form. A high oblique Gemini V photograph of the region shows several significant changes that have occurred since AMS 1:1,000,000 map NH-51 was compiled in 1955 (Figure 11). Rapidly changing features such as these emphasize the merit of a continuous earth orbital imaging program.

ERRORS OF PORTRAYAL

The second group of mapping discrepancies to be discussed involves errors of portrayal, defined as incorrect representation of any topographic features that is not, as far as can be determined, due to either man-made or geologic post-mapping changes. This type of mapping error is often the result of either incomplete or incorrect mapping data. It will be obvious that the distinction between these errors and those of post-mapping changes is at times arbitrary.

The first example of mapping error occurs in the intricate windings of a tributary of the Ucayali River in Peru, Rio Pachitea. A Gemini IX photograph of the area, taken in June, 1966, shows that Rio Puzzo, near Rio Pachitea and denoted as an unsurveyed stream on AMS 1:1,000,000 map SC-18, actually juts farther north and is less rounded in curvature than shown on the map (Figure 12). More striking is the similar analysis of Rio Burgararaco, also designated as unsurveyed. This river is clearly visible on the photograph, and is obviously too short and incorrectly drawn on the AMS map.

Additional errors in the same river system are observed one degree east on the succeeding photograph. Rio Ucayali, twisting methodically through the center of the photograph, is misrepresented in three principal places on AMS 1:1,000,000 SC-18 (Figure 13). First, the braided stream system between Rio Inuya and Rio Inchipachiaru is much broader than shown on the map. Second, the shape of the meandering river segment between the Peruvian cities of Pacaya and Curahuahia is markedly incorrect. Third, the Ucayali stream course is largely misplaced between Glas Chaguanya and Tarrbo de Caribos, as is obvious on the illustration. The errors in this and the previous example are probably due to post-mapping changes, with erosional and depositional variation in the stream course and migration of meanders having occurred. The map was copied in 1947, and the photograph was taken in 1966; this period is quite long enough for such major stream changes to have occurred.

Another area of cartographic interest, the northern half of Africa, has been almost completely photographed from manned orbital spacecraft. One of the

photos, taken over the circular Richat structures at the western fringe of the Sahara in Mauritania, is a notable example showing significant discrepancies that can occur between photograph and map. It is impossible to completely correlate all of the gross topographic features seen on a Gemini XII photo with AMS 1:1,000,000 maps NE, NF-28, 29, particularly at 13°W, 20°N (Figure 14). The massifs and rocky plateaus southwest of the Richat structures are incorrectly shown, but even more distressing is that the four maps do not coincide at their point of juncture. The relative reliability of the area is designated on NF-28 as poor, and the Gemini photograph seems to substantiate this description.

Cartographic problems also exist in the southern half of the continent, as evidenced with the study of Etosha Pan, Southwest Africa, from a Gemini VII photograph. Unfortunately, many of the photos taken on that flight were obscured by residue on the spacecraft window, and this particular exposure of the Pan is only about 60% usable. It does reveal, however, that the shape of the structure has been incorrectly portrayed on AMS 1:1,000,000 map SE 33 (Figure 15). Several other salt pans, smaller in size and located 13 miles west of Etosha Pan, are even less accurately shown. To the southwest, crustal flexures form impressive, longitudinal ridges which extend for at least 75 miles. These are not even indicated to exist on the AMS map, published in 1949.

One third the distance around the earth, Batan and Rapu-Rapu Islands, in the Philippines, provide us with a final example of mapping portrayal error. Channels between the islands and connecting Lagonoy and Tabaco Bays with Albay Gulf are shown as being much wider, relatively, on the AMS 1:1,000,000 map ND 51 than they appear on the Gemini V photograph of the area (Figure 16). About 35 miles north of these islands, on the Caramoan Peninsula, other mapping descrepancies exist; in particular, a short peninsula located between Bitaogan and Colongeocon and jutting into the Lagonoy Bay from Caramoan is not shown on the map. These discrepancies could be due to fluctuating tides. Oceanographic applications are also evident here.

ERRORS OF OMISSION

Now that some of the problems of topographic mapping have been demonstrated through the previous examples, the third and often surprising category, errors of omission, will be discussed. These are defined as instances where topographic features of significant dimension have been completely omitted from the map. As in the previous examples, map obsolescence and lack of adequate source material play a major part in these discrepancies.

The initial example to be considered is one of surprising magnitude and geologic importance. The Palomas volcanic field in northern Chihuahua,

Mexico, lies immediately south of the New Mexico border and covers over 200 square miles. A Gemini IV photograph, one in a series across the southwestern U. S. and northern Mexico, shows the field to be readily discernible from space and to contain over 30 cinder cones or vents (Figure 17). Most of these cones have been breached and range between 100 and 400 feet high (Lowman, 1969). Despite these large and distinguishing features, contemporary geologic and topographic maps fail to illustrate this volcanic field (e.g., "Geologic Map of N. America", E. M. Goddard, 1965, USGS). Because of the low height of the volcanoes in the field, they are relatively inconspicuous from ground level, and this may partially account for its omission from maps of the area. Nevertheless, omissions of this magnitude effectively illustrate the unreliable state of some contemporary published topographic maps.

Another large and striking error of omission is seen with a Gemini V shot of Lake Titicaca, Bolivia. A mound-shaped Tertiary volcanic plug on the southwestern side of the lake spans over 100 square miles in area and is prominent in appearance from space, yet is not shown on AMS 1:1,000,000 map SE-19 (Figure 18). Further, the southern shoreline of Lake Titicaca and the shape of Laguna de Uinamarca are incorrectly plotted. Concordant with these distortions, the Peninsula de Copacabana, which separates the two water bodies, is not accurately shown. Map source data, from an AGS 1922 map, is apparently obsolete.

Continuing east to Africa, another interesting area is seen northeast of the extensive Tibesti massif of North-Central Africa. Numerous rocky uplifts are sharply contrasted against a background of sand on Gemini XI synoptic photographs of the area. Reference to AMS 1:1,000,000 map NF-34, 35 indicates that the structures are inadequately shown, if shown at all (Figure 19). In fact, it is virtually impossible to correlate some features clearly visible on the photo with the maps. Pesce (1968) describes two previously unmapped topographic features in this region, the Erg Idrisi and the Hamada Ibn Battutah. North of these structures, the El Cufra area is equally invalid on the AMS maps. The maps were compiled in 1956, and are designated as being based on source data of poor reliability.

The final example of error of omission to be considered here, which is also related to oceanography, is found west of Madagascar with the tropical Comoro Islands. Amid overhanging cumulus clouds and a bright glitter pattern upon the water, a distinct coral reef is seen on a Gemini VI photo to encircle Mayotte Island. However, the structure is completely omitted on AMS 1:1,000,000 map SC-38, compiled in 1955 (Figure 20). The reliability of the area is given as fair, and is based upon small scale hydrographic charts.

SUMMARY AND CONCLUSIONS

These 20 examples of mapping errors, including post-mapping changes, errors of portrayal, and errors of omission, indicate the wide range of discrepancies that can be recognized when comparing orbital photographs and published topographic maps. The orbital photographs can make a significant contribution to the correction and continuous updating of these maps. Specifically, they can provide global coverage of the earth, within flight path restrictions, an especially important asset to mapping remote areas. Also, orbital photography offers rapid repetition of coverage and thus a partial solution to the problem of post-mapping changes. These advantages, coupled with the large area per photo, availability of color imagery, and wide range of scales, describe the potential usefulness of orbital photography to the task of world-wide mapping.

ACKNOWLEDGEMENTS

Contributors to the development of this report and the collection of data upon which it is based are numerous. Foremost are the astronauts, whose successful completion of the Synoptic Terrain Photography (S-005) Experiment and the Synoptic Weather Photography (S-006) Experiment has provided us with this expansive view of the earth. Dr. Paul D. Lowman, Jr., of Goddard Space Flight Center, stimulated the construction of this report, and without his diverse and expert advice its completion would not have been possible. Herbert Blodget, also of Goddard, provided many valuable suggestions and ideas for the paper. Herbert Tiedemann and Richard Underwood, of the Manned Spacecraft Center, Houston, provided much of the basic data for this research by making preliminary photograph identification and data assessment.

REFERENCES

1. Atwood, Wallace W. The Physiographic Provinces of North America. Boston: Ginn and Company, 1940.

2. Darwin, George Howard. The Tides and Kindred Phenomena in the Solar System. San Francisco: W. H. Freeman and Company, 1962, pp. 221-250.

3. Doyle, Frederick J. "Mapping from Satellite Photography." Distinguished Scientist Presentation Sponsored by American Society of Photogrammetry & National Science Foundation (1967-).

4. Gilluly, James, et al. Principles of Geology. 3rd ed. San Francisco: W. H. Freeman and Company, 1968.

5. Holmes, Arthur. Principles of Physical Geology. New York: Ronald Press Company, 1965.

6. Jaeger, Edmund C. The North American Deserts. Standord: Stanford University Press, 1957.

7. Krumbein, W. C., and L. L. Sloss. Stratigraphy and Sedimentation. San Francisco: W. H. Freeman and Company, 1951.

8. Lowman, P. D. "Geologic Orbital Photography: Experience from the Gemini Program." Photogrammetria, 24 (1969), pp. 77-106.

9. Munk, Walter H. and Gordon J. F. MacDonald. Rotation of the Earth. Cambridge: University Press, 1960.

10. National Geographic. Atlas of the World, ed. Melville Bell Grosvenor. Washington, D. C.: National Geographic Society, 1963.

11. Pesce, Angelo. Gemini Space Photographs of Libya and Tibesti. Tripoli: Petroleum Exploration Society of Libya, 1968.

12. Rusnak, Gene A. "Sediments of Laguna Madre." Recent Sediments, Northwest Gulf of Mexico. ed. Francis P. Shepard et al. Tulsa: American Association of Petroleum Geologists, 1960.

13. Scientific and Technical Information Division, Office of Technology Utilization; NASA. Earth Photographs from Gemini III, IV, and V. Washington, D. C.: NASA Headquarters, 1967.

14. Shepard, Francis P. "Continental Shelf Sediments." Recent Marine Sediments, ed. Parker D. Trask. New York: Dover Publications, Inc., 1955.

15. Smith, H. T. U. Photo-Interpretation Studies of Desert Basins in Northern Africa. Bedford: Air Force Cambridge Research Laboratories, 1969.

16. Times Atlas of the World. ed. John Bartholomew. Boston: Houghton Mifflin Company, 1958.

17. Thornbury, William D. Principles of Geomorphology. 2nd ed. New York: John Wiley and Sons, Inc., 1969.

LOCATIONS OF PHOTOGRAPHS


17
1
2
3
5
12
18
18
4

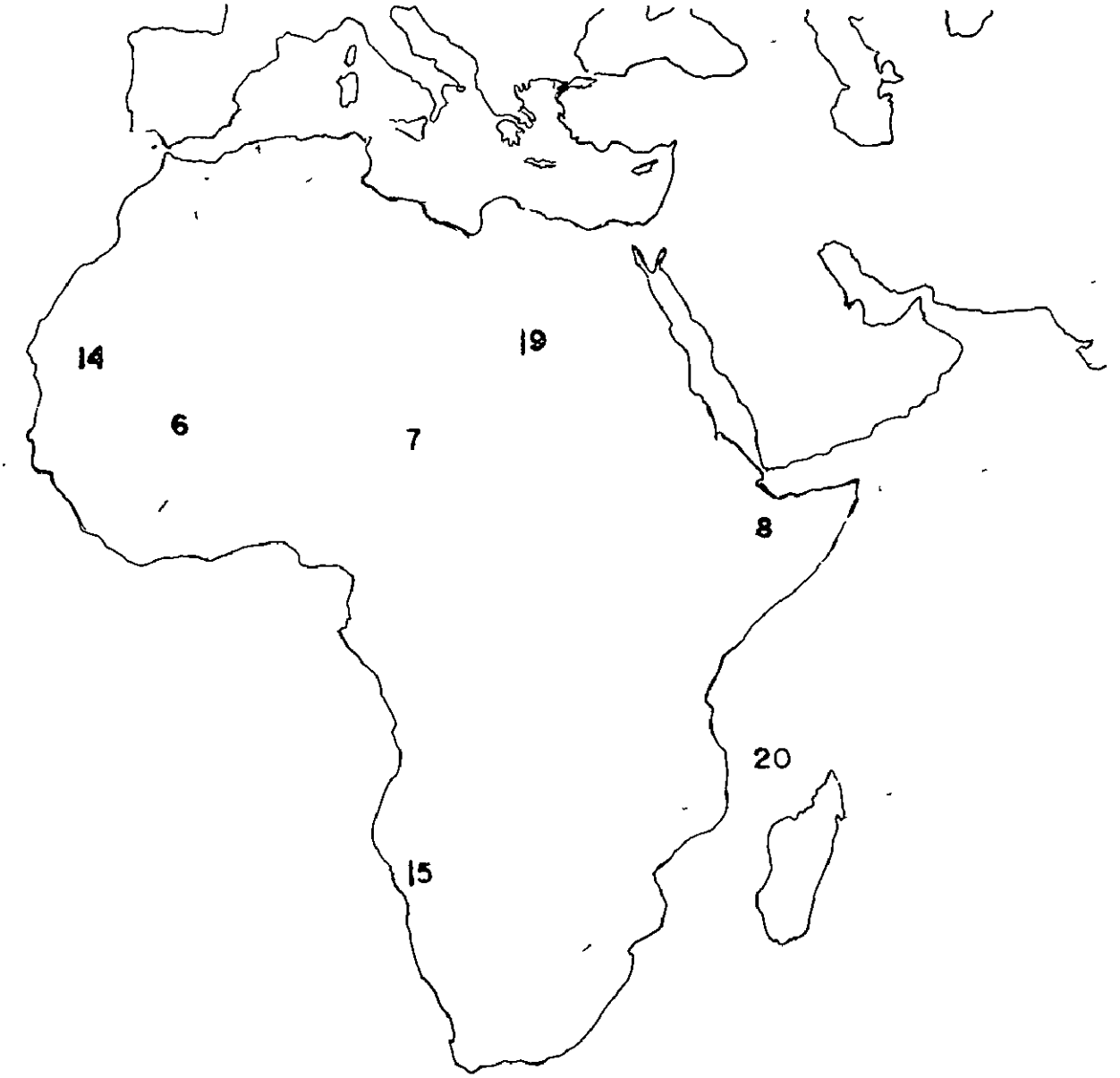
14
19
6
7
8
20
15


9
10
11
16

a. Gemini V, S-65 - 45699

Figure 1. Gemini V, VII photographs S-65 - 45699, S-65 - 63871 of Punta Eugenia (A) and Laguna Ojo de Libre (B), Baja California. The former shot was taken on August 21, 1965, and the latter on December 8, 1965. Distance between arrow points is 15 statute miles.

b. Gemini VII, S-65 - 63871

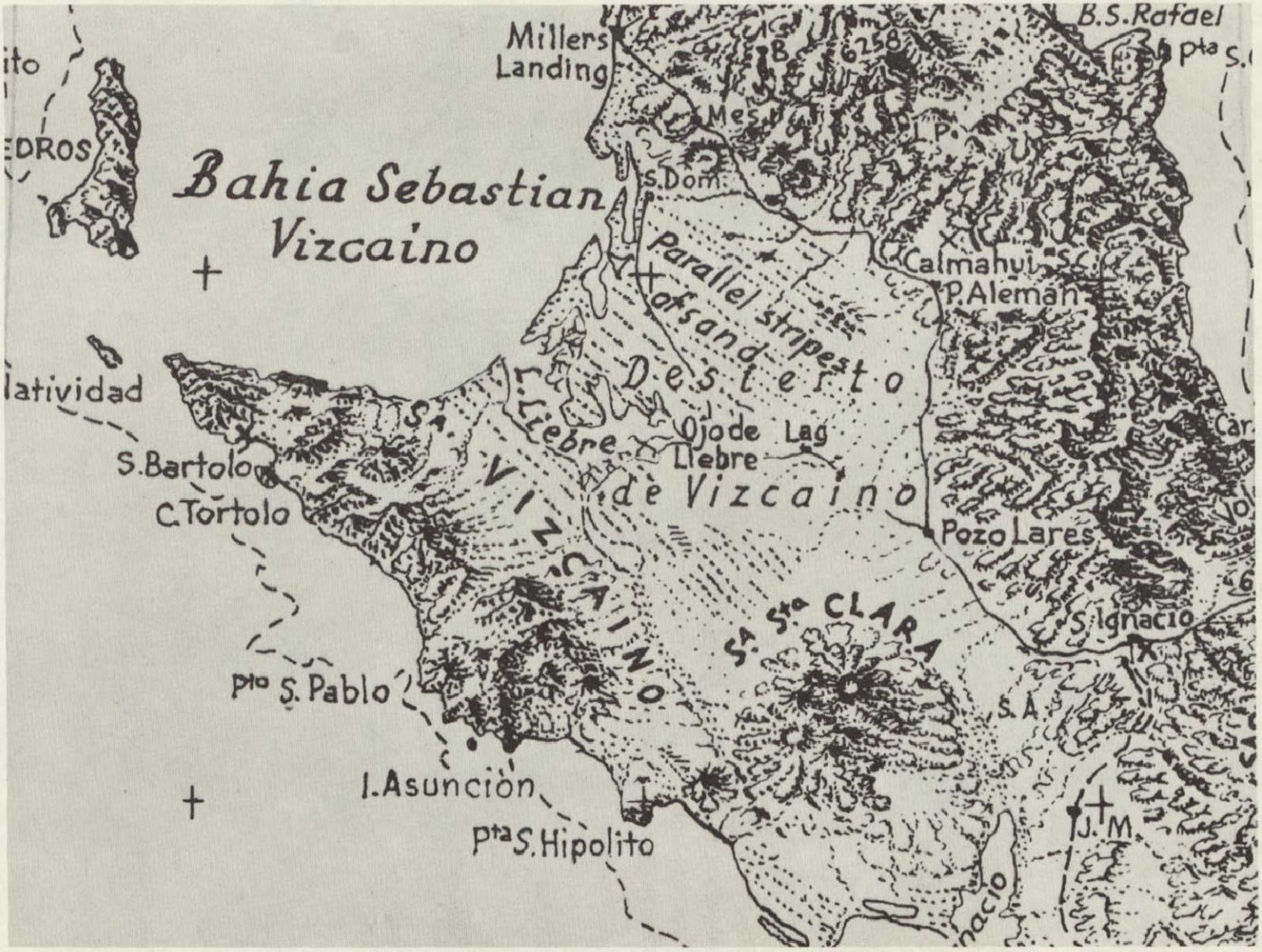

c. Enlarged Portion of Landform Map of Mexico, by Irwin Raisz

Figure 2. Gemini V photograph S-65 - 63760 shows 3-petalous President Benito Juarez Dam, Oaxaco, Mexico (center, arrow). To the right is Laguna Superior (A). Distance between arrow tip at reservoir and letter A represents 31 statute miles on photograph.

a. Gemini V, S-65 - 63760

b. AMS NE-15, 1:1,000,000, Enlarged Portion

Figure 3. Gemini V photograph S-65 - 45705, of the Coco River (left center), and Laguna Caratasca (upper center). Honduras and Nicaragua lie north and south, respectively, of the river. Distance between arrow tips is 19 statute miles. Cloud coverage is considerable. Photograph is oblique view to south.

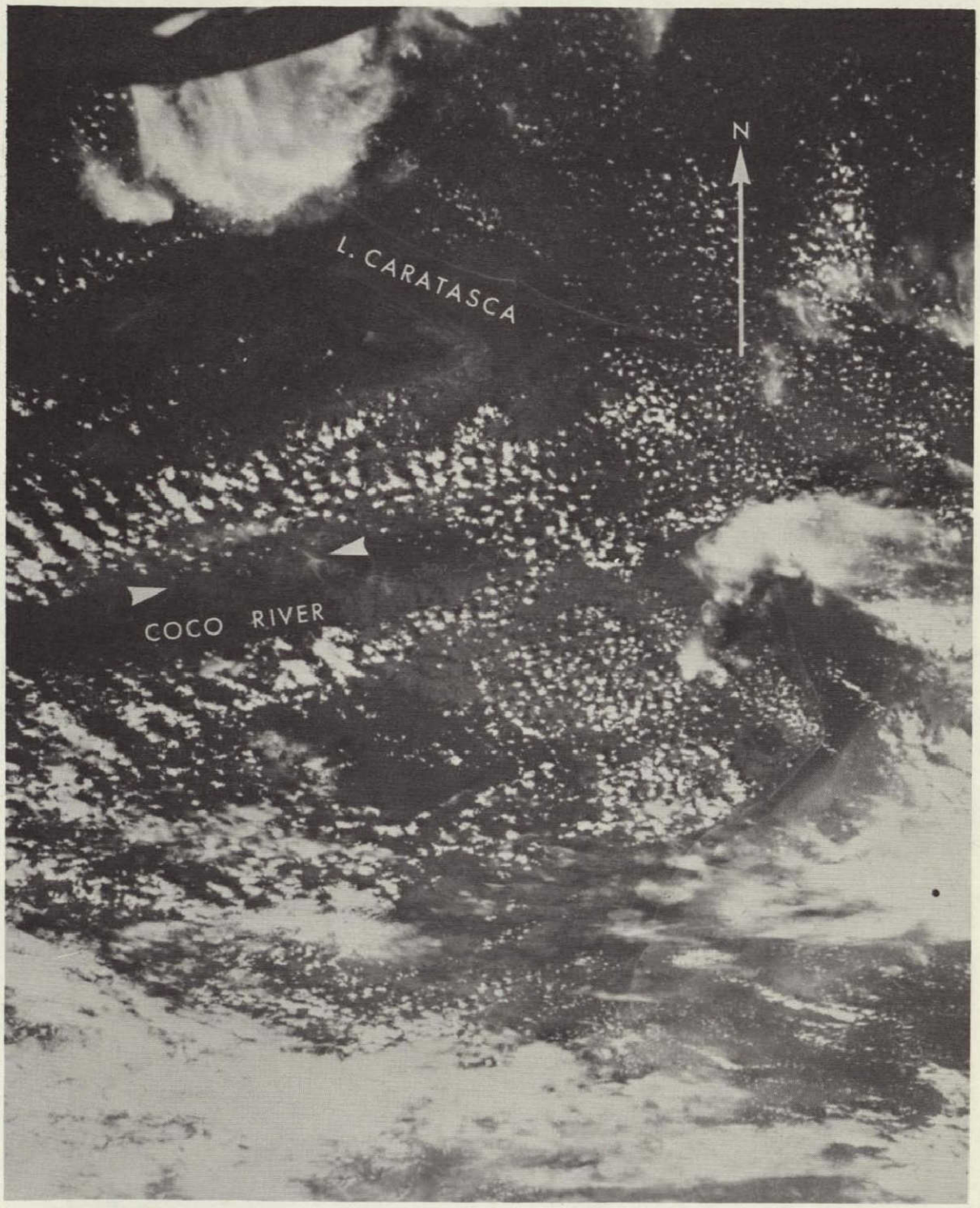

a. Gemini V, S-65 - 45705

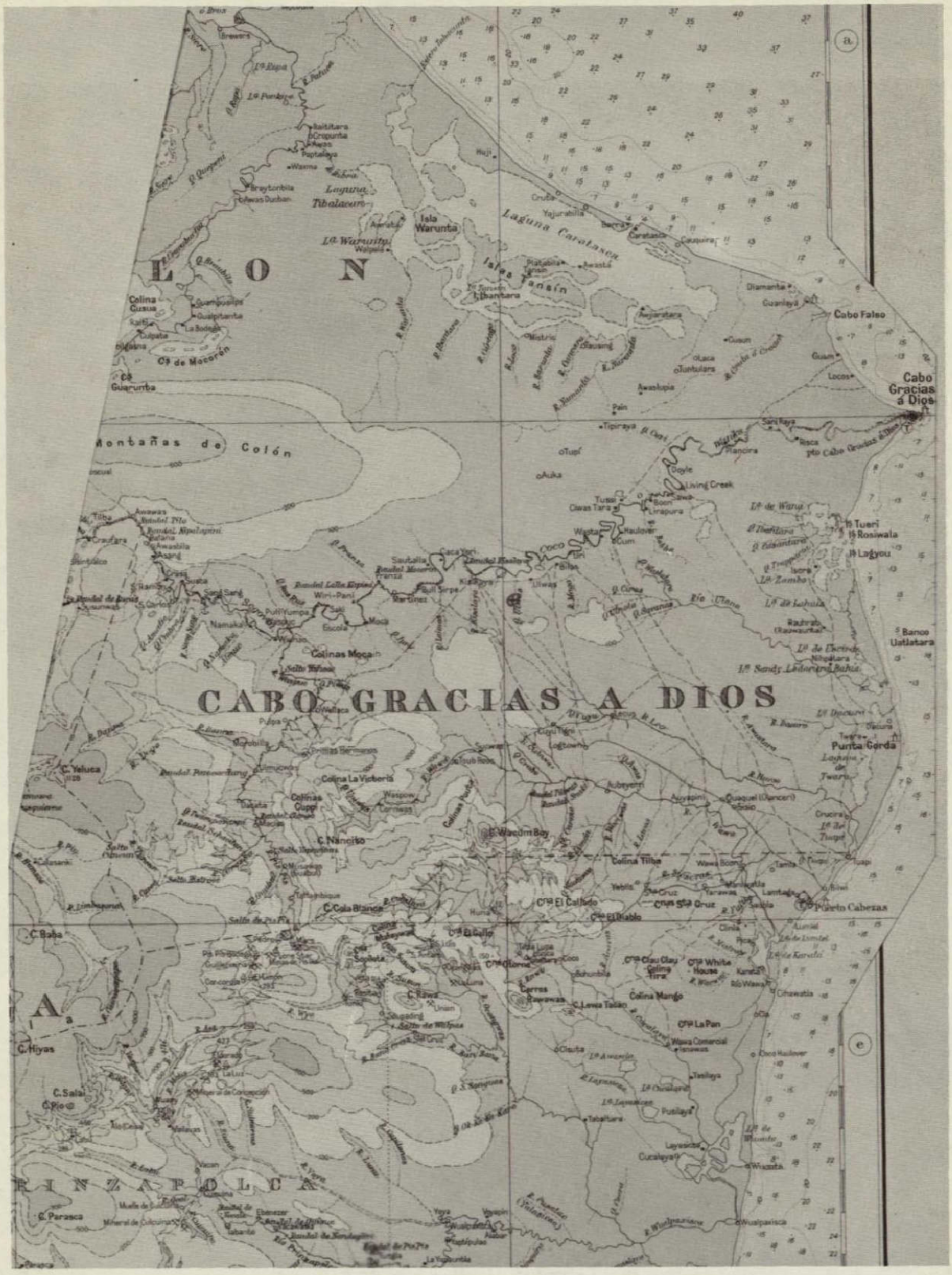

b. AMS ND-16, 1:1,000,000, Enlarged Portion

Figure 4. Gemini V photograph S-65 - 45613, of Lago de Poopo (A) in Oruro Potosi, Bolivia. Unmapped lake is in upper center of photograph (arrow). Gemini IX photograph S-66 - 38313 provides a supplemental oblique view of the area, looking south from Lake Titicaca (right, B). Two large salt playas, Salar de Coipasa (C) and Salar de Uyuni (D), lie southwest of Lago de Poopo. Adjacent to the playas is Lago de Coipasa (arrow, on the GT-IX photo). Distance between lakes Titicaca and Poopo is approximately 150 statute miles.

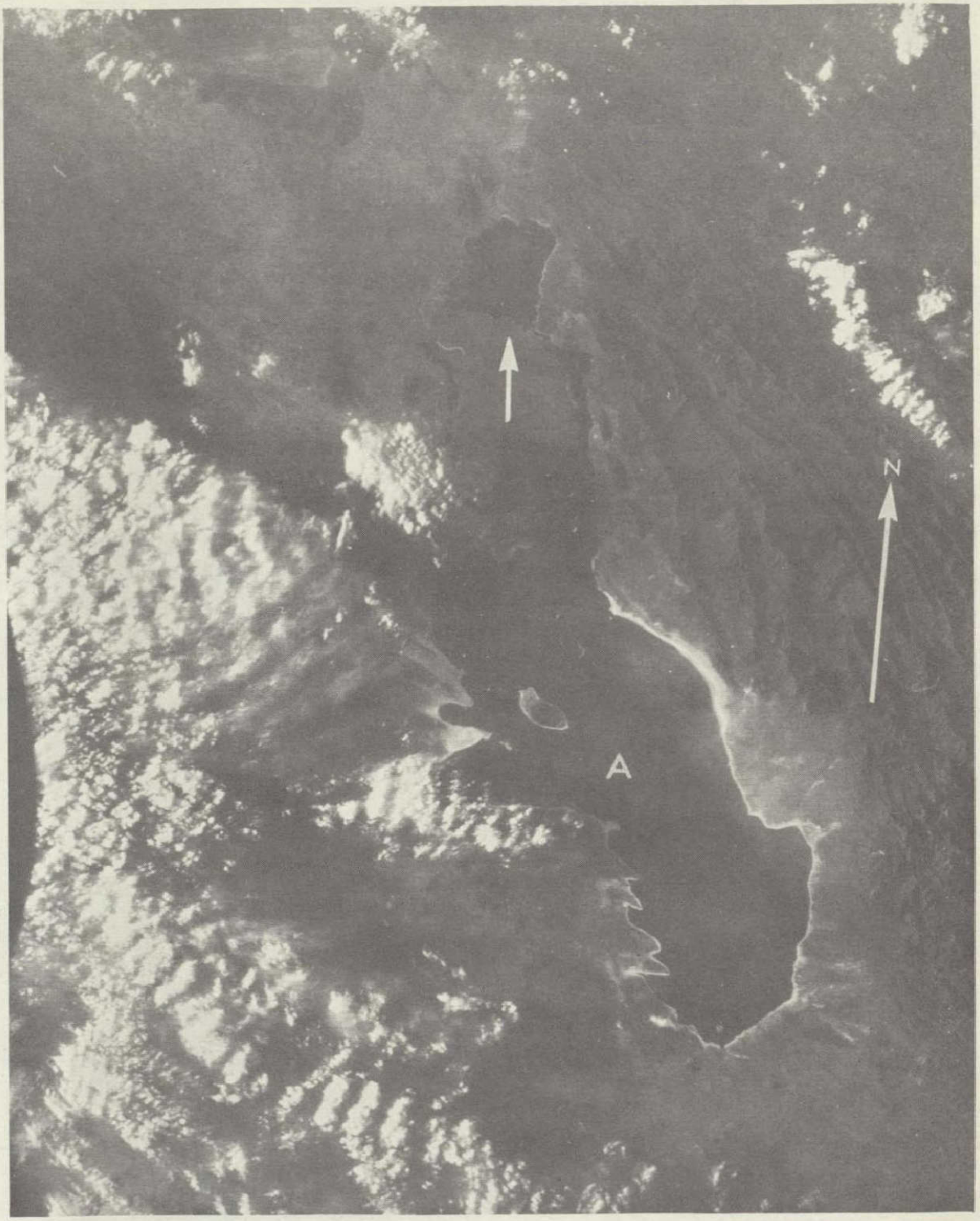

a. Gemini V, S-65 - 45613

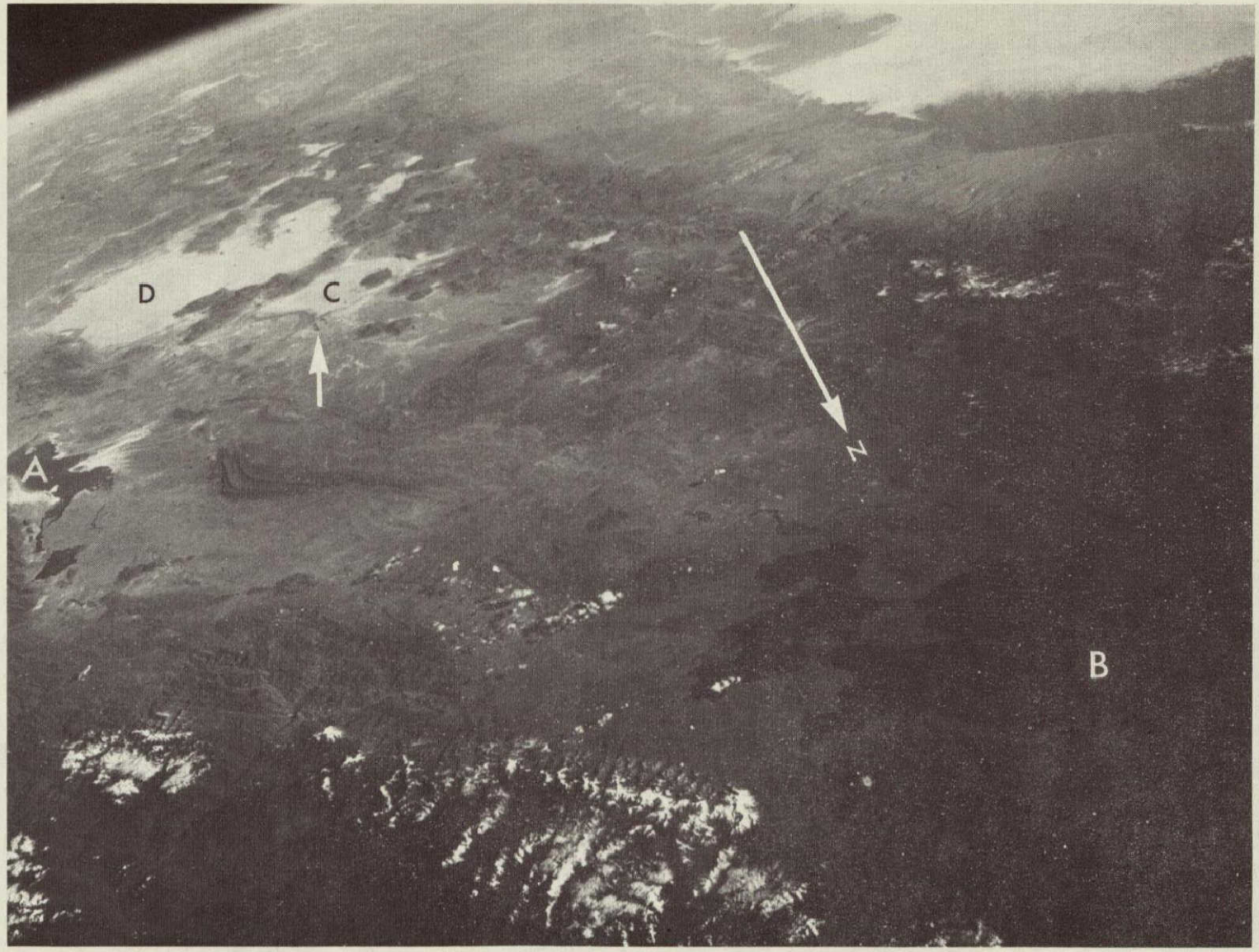

b. Gemini IX, S-66 - 38313

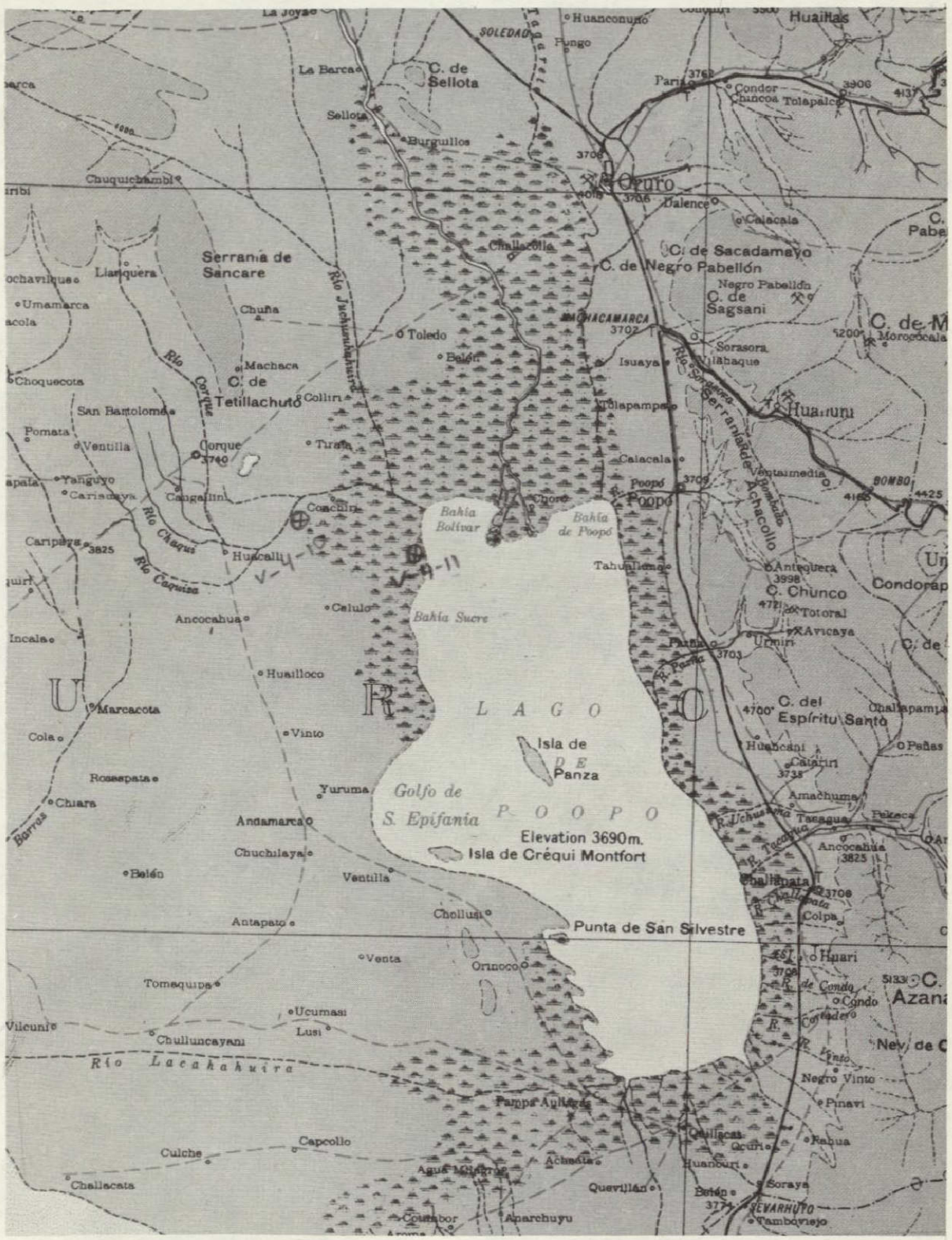

c. Enlarged Portion of AMS SE-19, 1:1,000,000

Figure 5. Gemini VII photograph S-65 - 64001, of Amazon River mouth. Four areas of map error discussed in text are denoted by arrows on the photograph. North arrow length represents 22 statute miles on photograph.

a. Gemini VII, S-65 - 64001

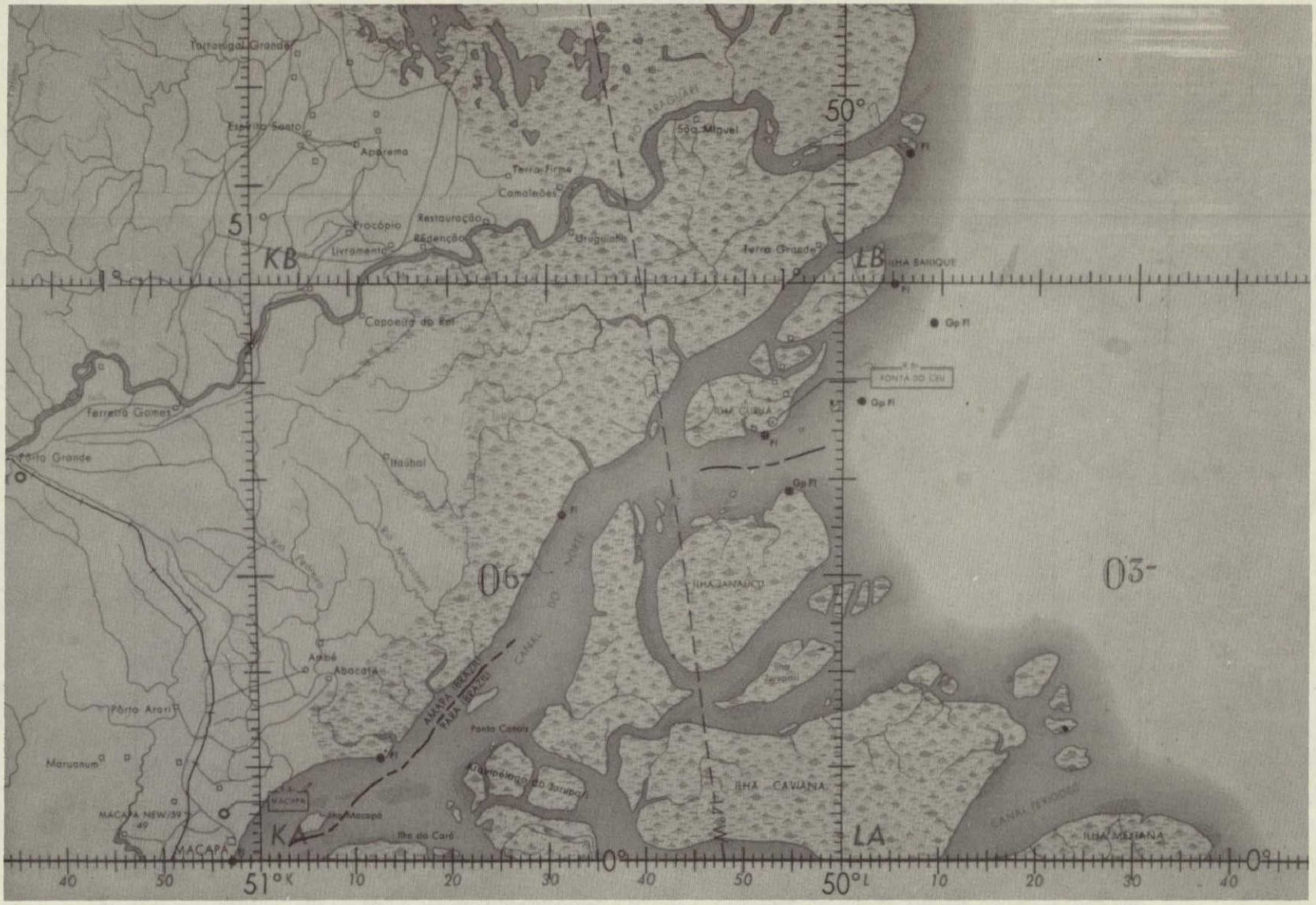

b. AMC Hydrographic Chart L-28, 1:1,000,000, Enlarged Portion

Figure 6. Gemini VI photograph S-65 - 63246, of Niger River, Mali. Surrounding area is marsh, subject to flooding. Tombouctou shown by arrow. Distance between two parallel arrow tips on photo is 15 statute miles.

a. Gemini VI, S-65 - 63246

b. AMS NE-30, 1:1,000,000, Enlarged Portion

Figure 7. Gemini IX photograph S-66 - 38444, of Lake Chad. Dillia sebkha is at top (arrow). Distance between small, parallel arrow tips is 22 statute miles.

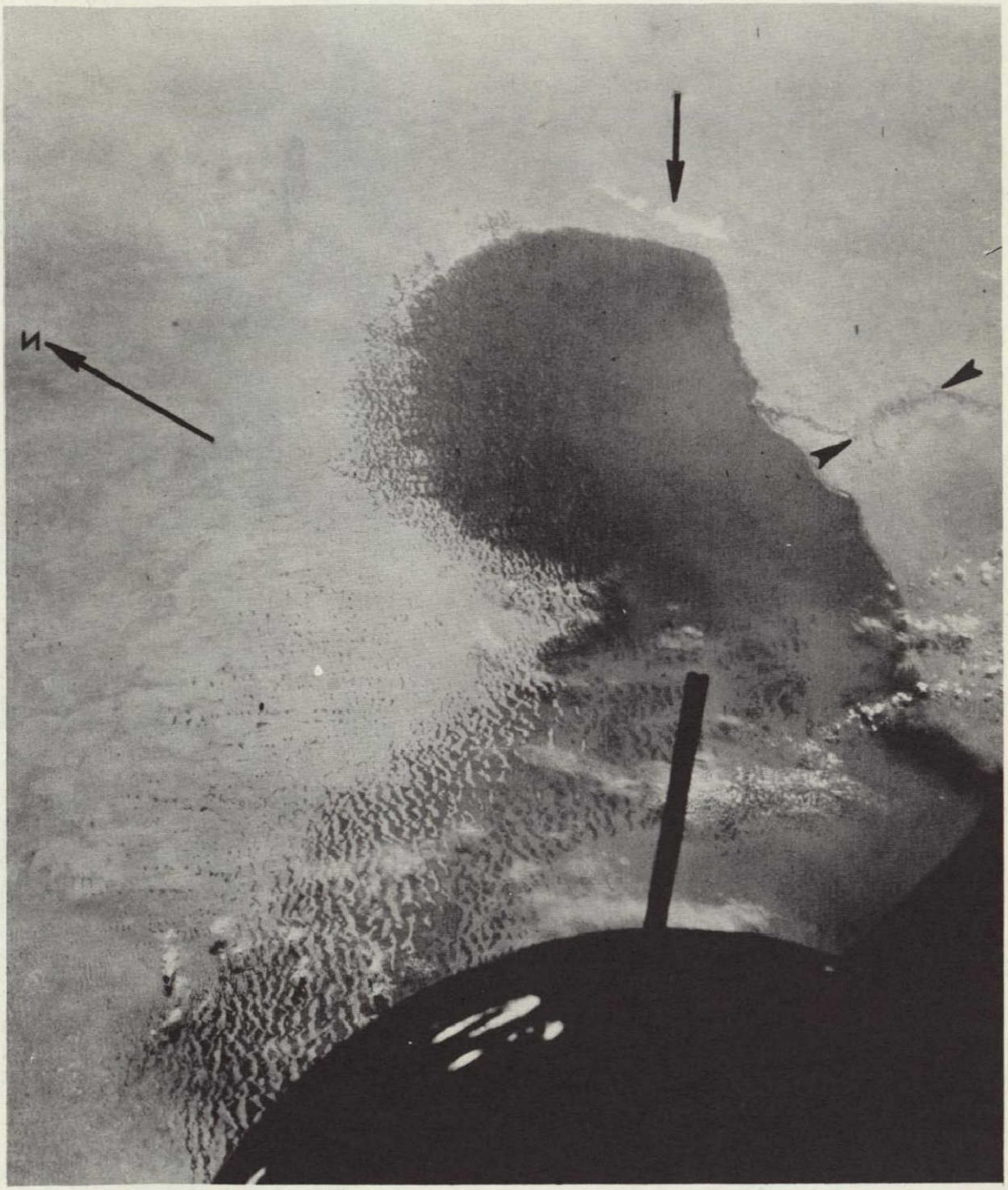

a. Gemini IX, S-66 - 38444

b. AMS ND-33, 1:1,000,000, Enlarged Portion

Figure 8. Gemini VI photograph S-65 - 63162, area south of Addis Abeba, Ethiopia. Two unmapped lakes are notated (arrows, upper right and lower center left). Width of Lake Langanno (west-east dimension) is approximately 10 statute miles.

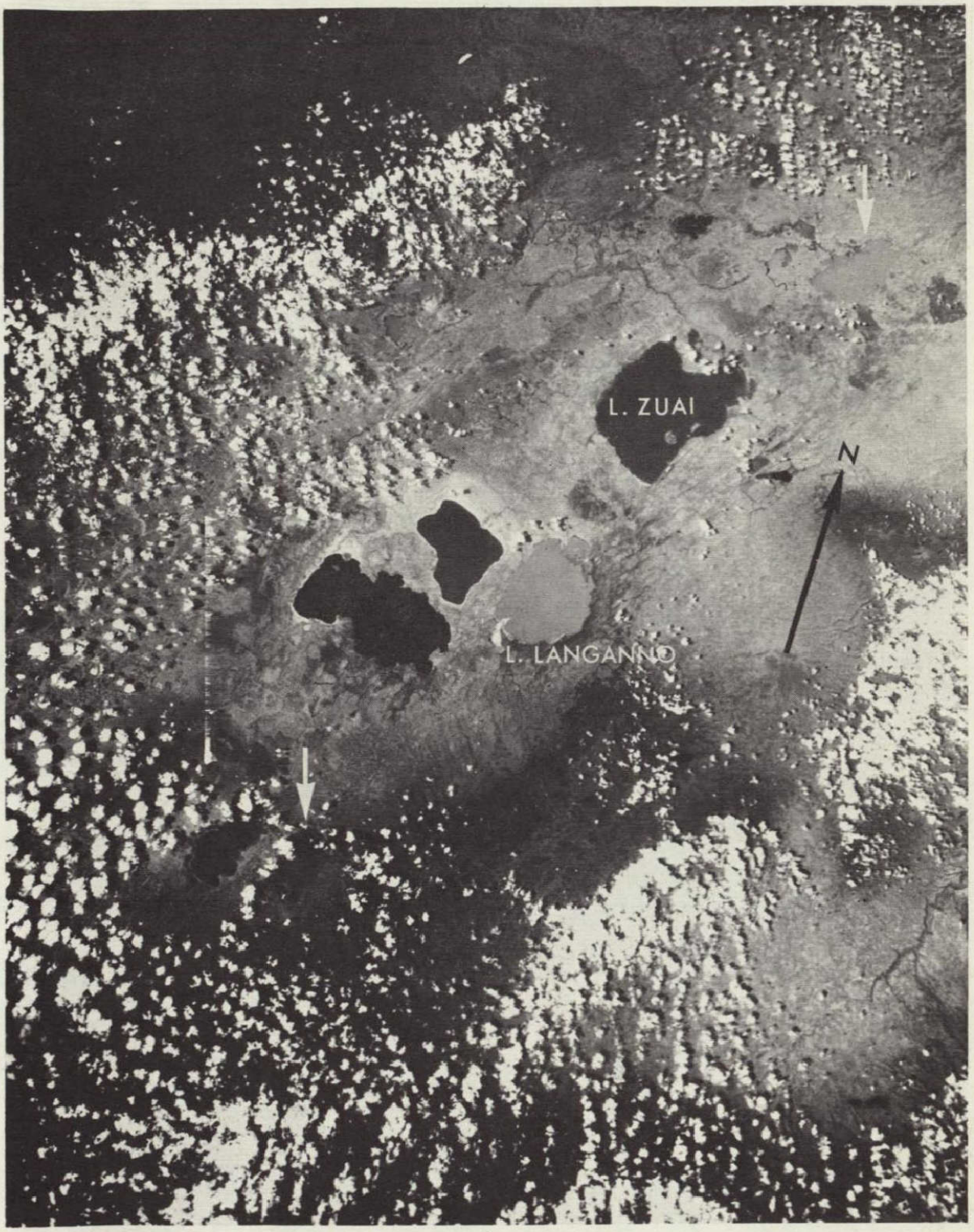

a. Gemini VI, S-65 - 63162

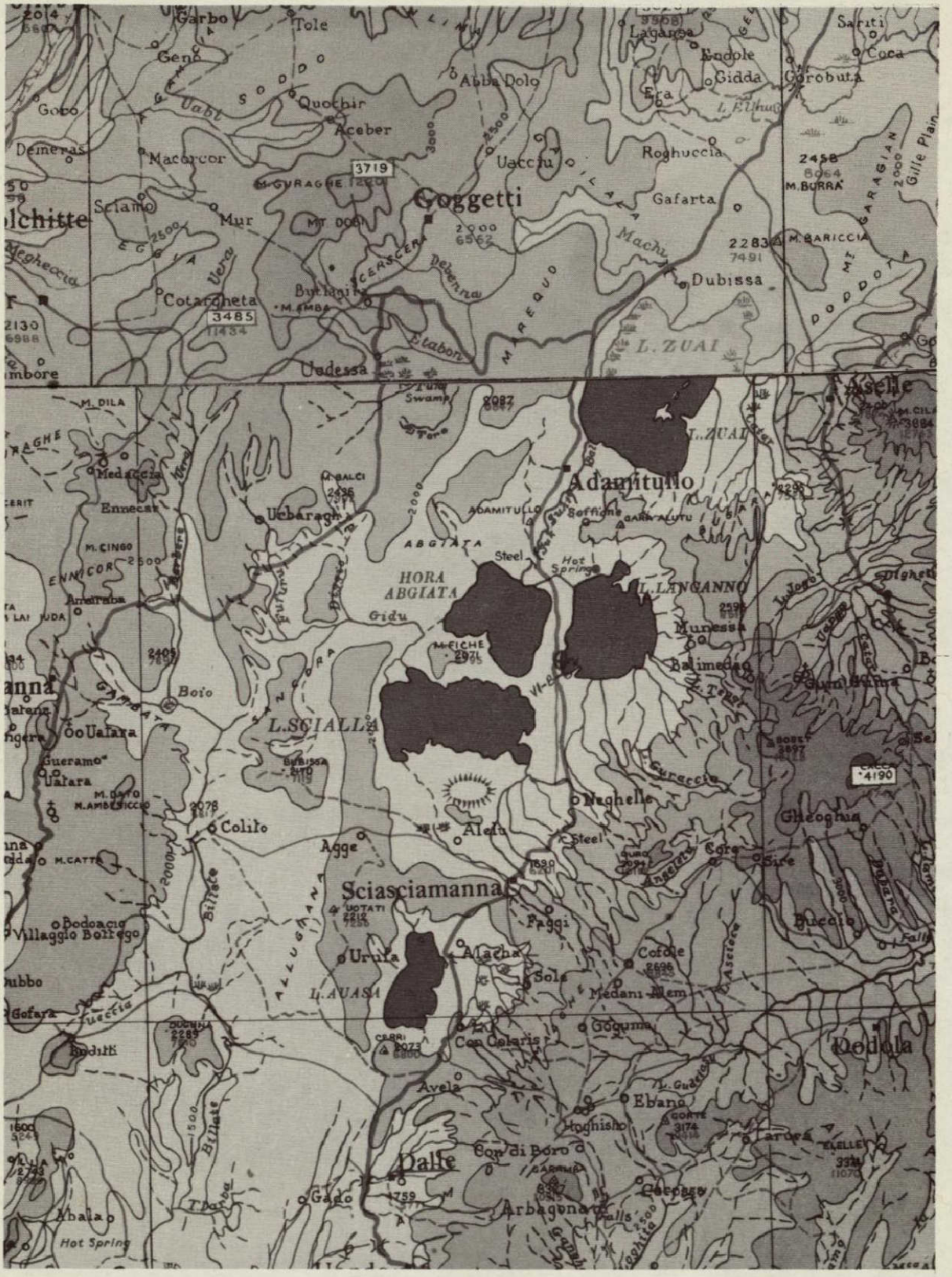

b. AMS NB, NC-37, 1:1,000,000, Enlarged Portions

Figure 9. Gemini V photograph S-65 - 45775, of Tibetan Plateau includes Charol Tsho (A) and Keze Tsho (B) under extensive cloud coverage. Distance between lakes is about 35 statute miles.

a. Gemini V, S-65 - 45775

b. AMS NI-44, 1:1,000,000, Enlarged Portion

Figure 10. Gemini V photograph S-65 - 45624 and Apollo 7 (AS7-5-1617) photographs of Tibet show Nganglaring Tso (A), Shovo Tso (B), Tabia Taska (C), Poru Tso (D), and Tarok Tso (E). Differences between photographs are most notable within Nganglaring Tso. Distance between Nganglaring Tso and Poru Tso is approximately 50 statute miles.

a. Gemini V, S-65 - 45624

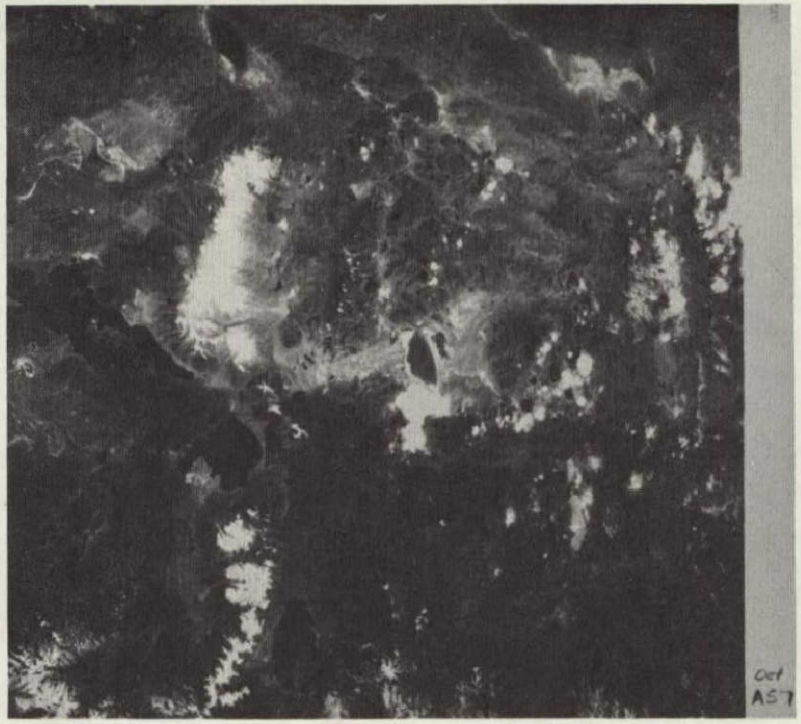

Apollo 7, AS7 - 5 - 1617

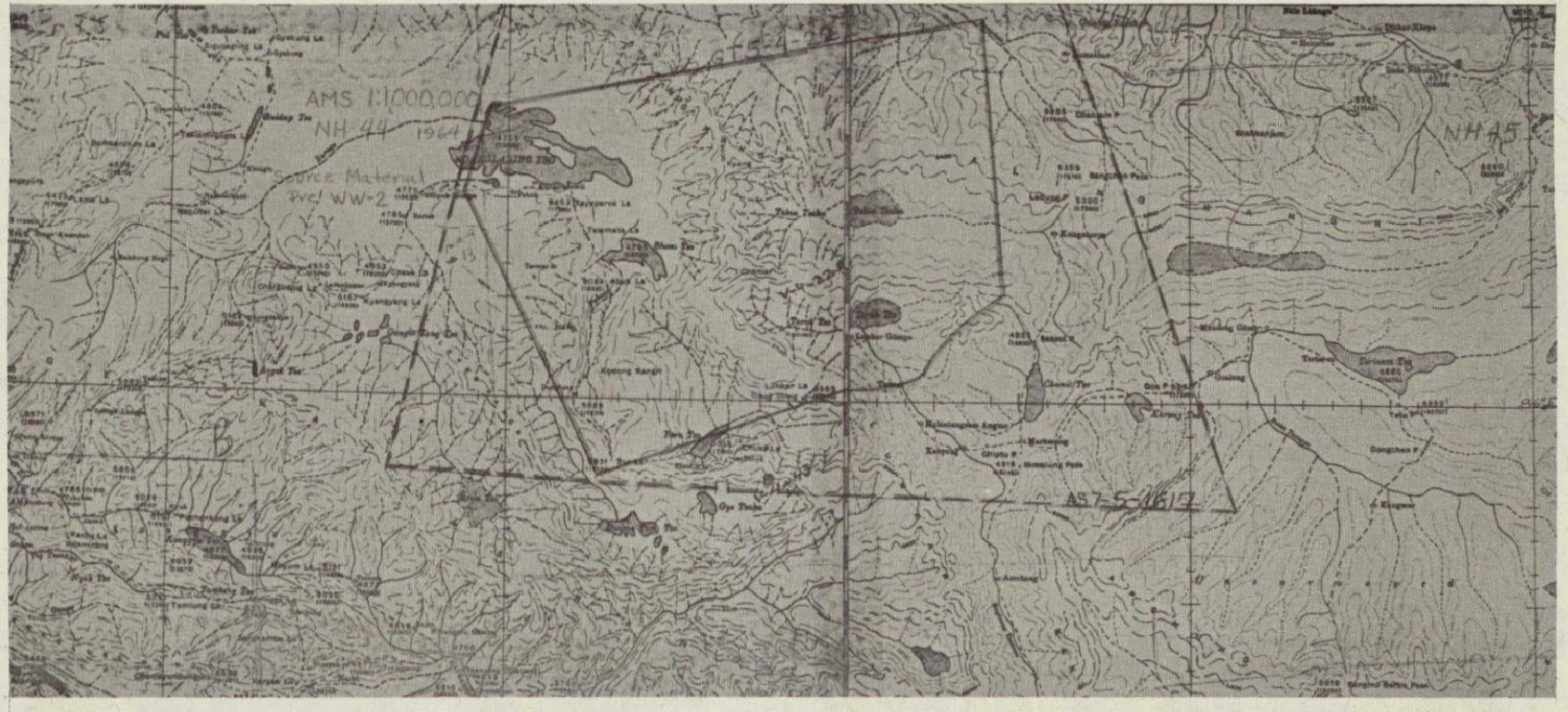

b. AMS 1:1,000,000 Maps NH-44, 45, Enlarged Portions

a. Gemini V, S-65 - 45768

Figure 11. Gemini V photograph S-65 - 45768, of Yanztse River mouth, China. Ch'ung-ming Tao (A) and city of Shang-hai (arrow) are denoted. Significant changes in island shapes are indicated with small arrows. Distance between Shang-hai and Ch'ung-ming Tao is about 20 statute miles.

b. AMS NH-51, 1:1,000,000, Enlarged Portion

Figure 12. Gemini IX photograph S-66 - 38301, of Ucayali River tributaries, Peru. Indicated are Rios Pachitea (C), Pozuzo (B), and Burgararaco (A). Town of Puerto Victoria is located by arrow. Distance between Puerto Victoria and letter C represents about 20 statute miles on photograph.

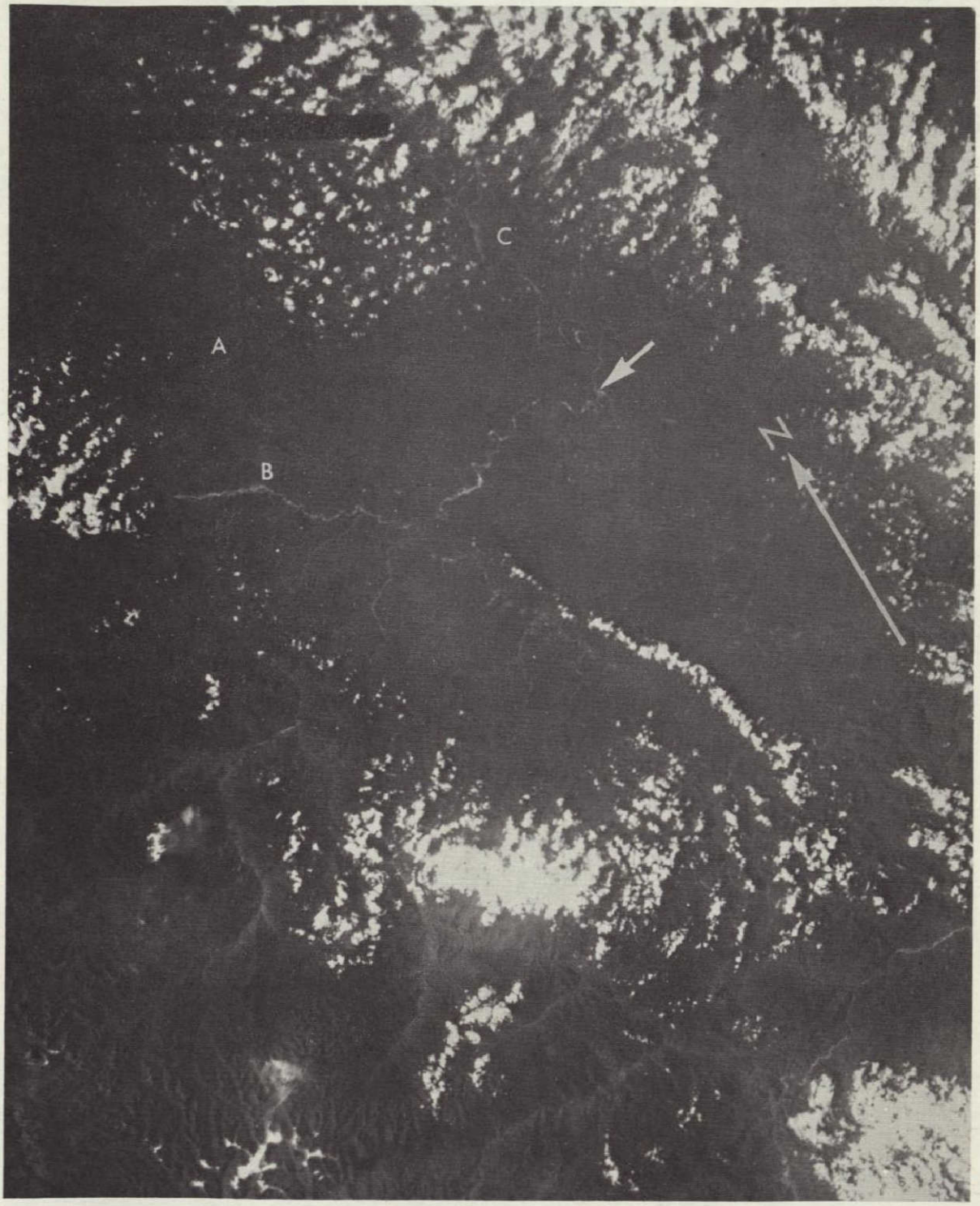

a. Gemini IX, S-66 - 38301

b. AMS SC-18, 1:1,000,000, Enlarged Portion

Figure 13. Gemini IX photograph S-66 - 38302, of Ucayali River tributaries one degree east of Figure 12. Three map errors referred to in text are numbered 1, 2, 3, respectively, on the photograph. Distance between numbers 1 and 2 represents approximately 37 statute miles.

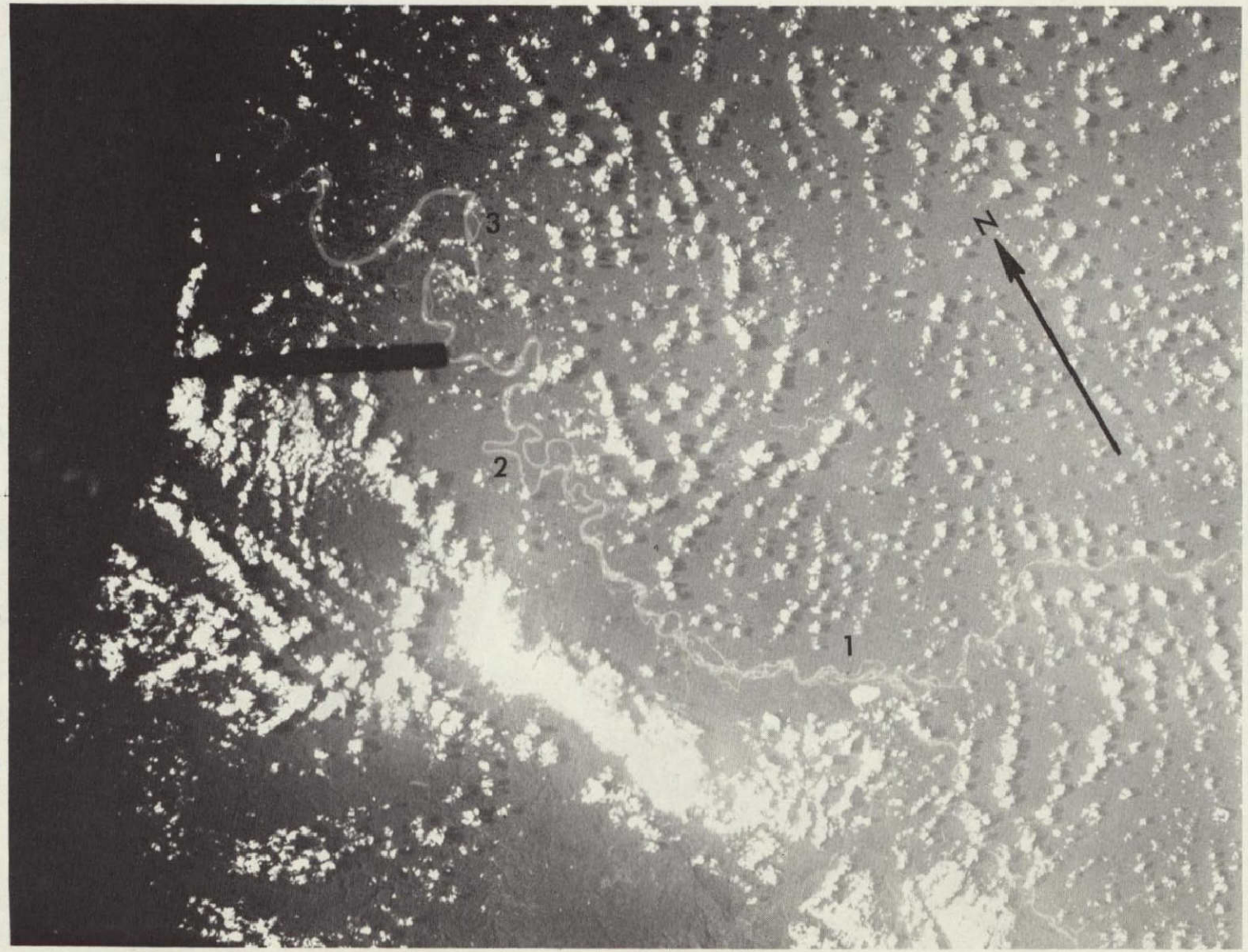

a. Gemini IX, S-66 - 38302

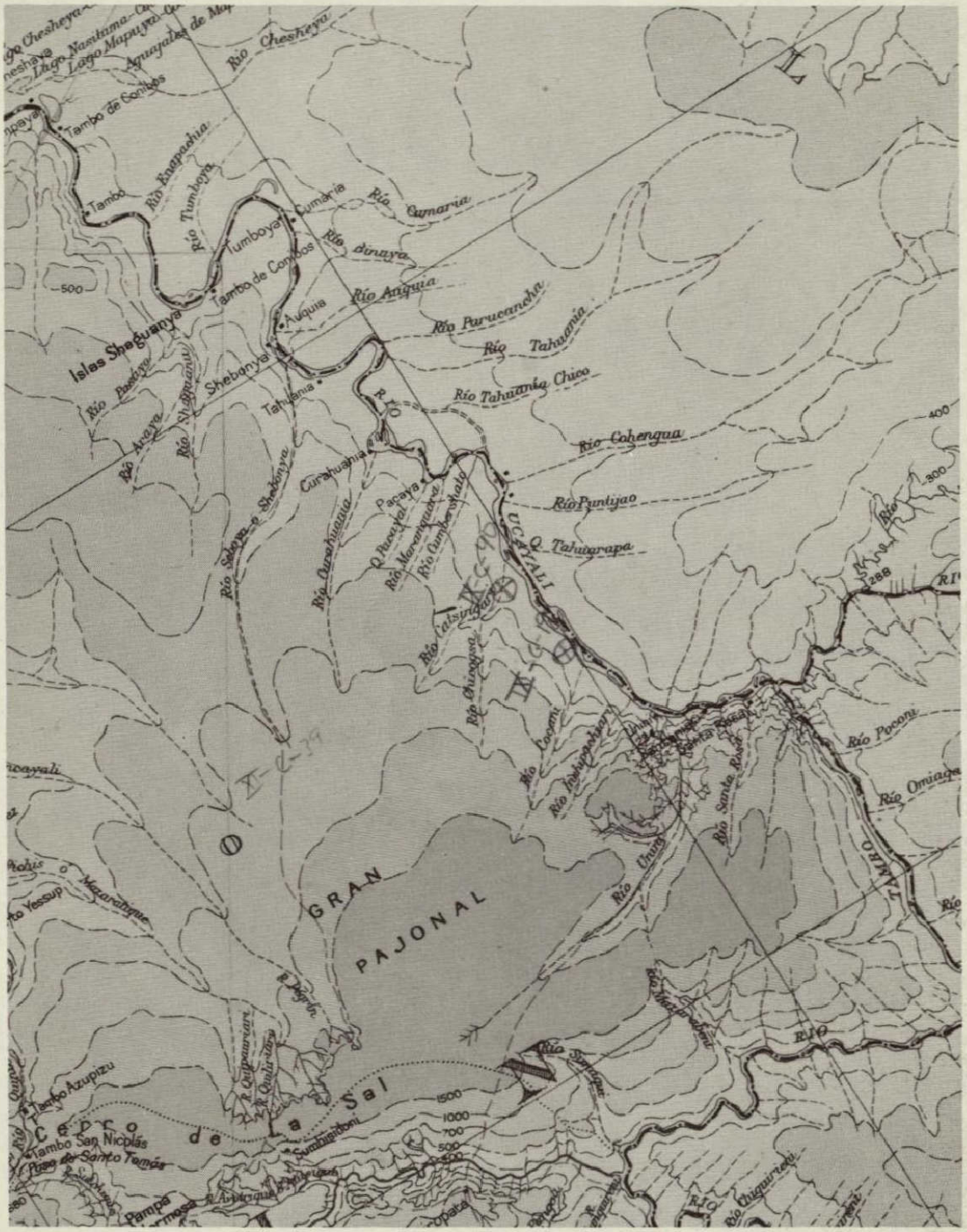

b. AMS SC-18, 1:1,000,000, Enlarged Portion

Figure 14. Gemini XII photograph S-66 - 63472, of Mauritania. Area containing the map error referred to in text is shown by box. Diameter of Richat structure (R) is about 24 statute miles.

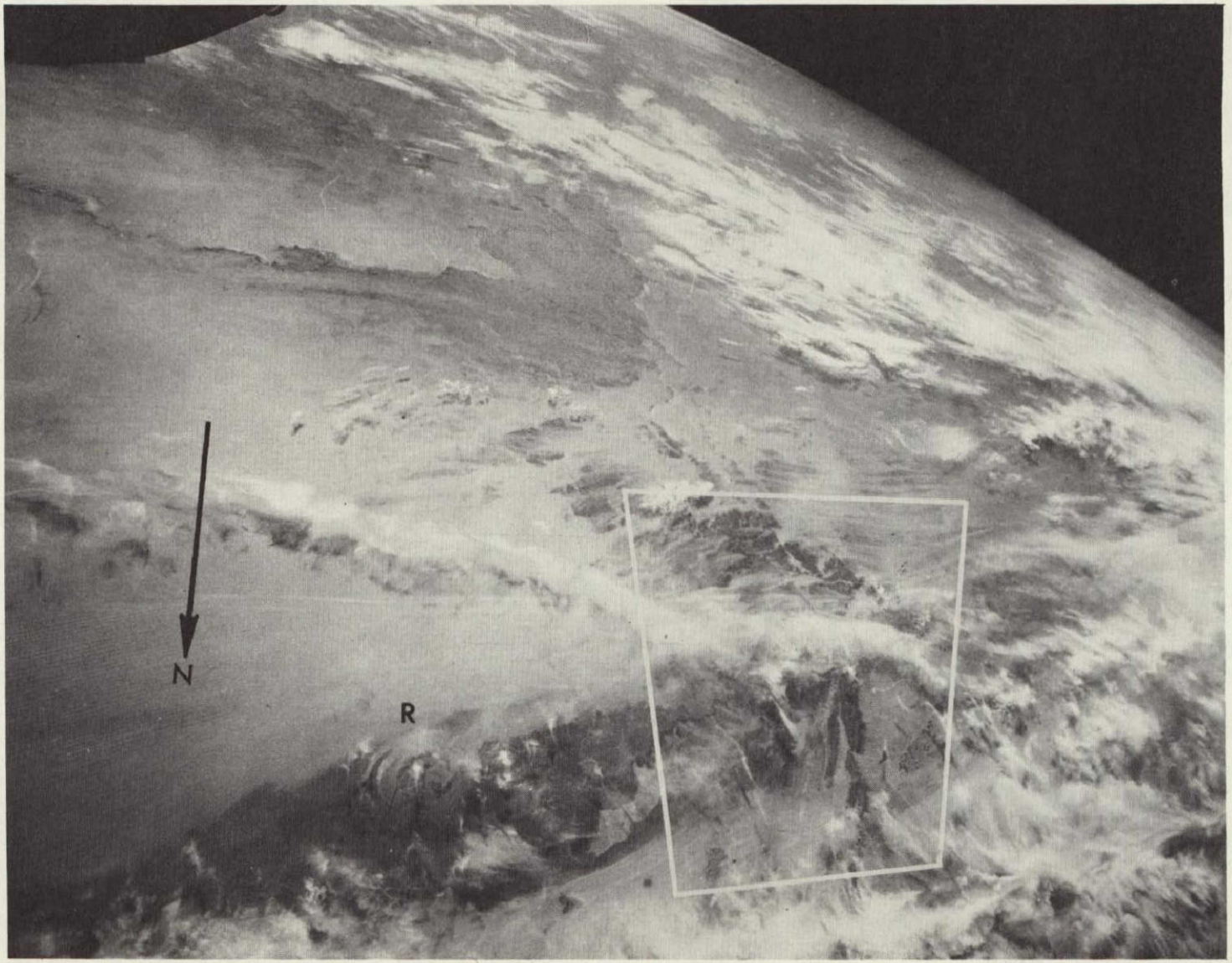

a. Gemini XII, S-66 - 63472

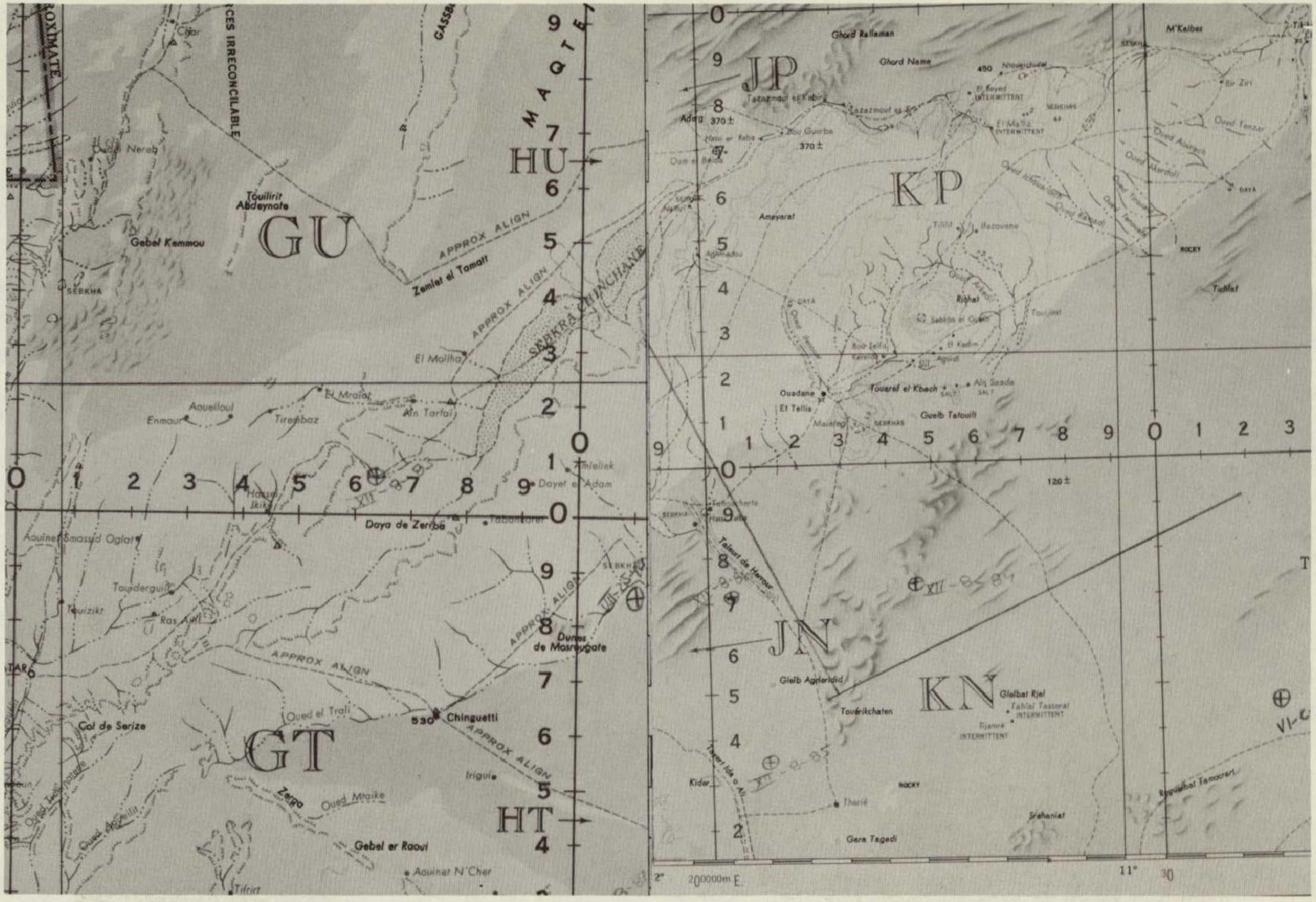

b. AMS NF-28, 29, 1:1,000,000, Enlarged Portions

Figure 15. Gemini VII photograph S-65 - 63911, of Etosha Pan (lower right, A), Southwest Africa. Smaller salt pans (center) and longitudinal ridges (lower left) referred to in text are visible, despite window residue. North arrow represents 20 statute miles on photograph.

a. Gemini VII, S-65 - 63911

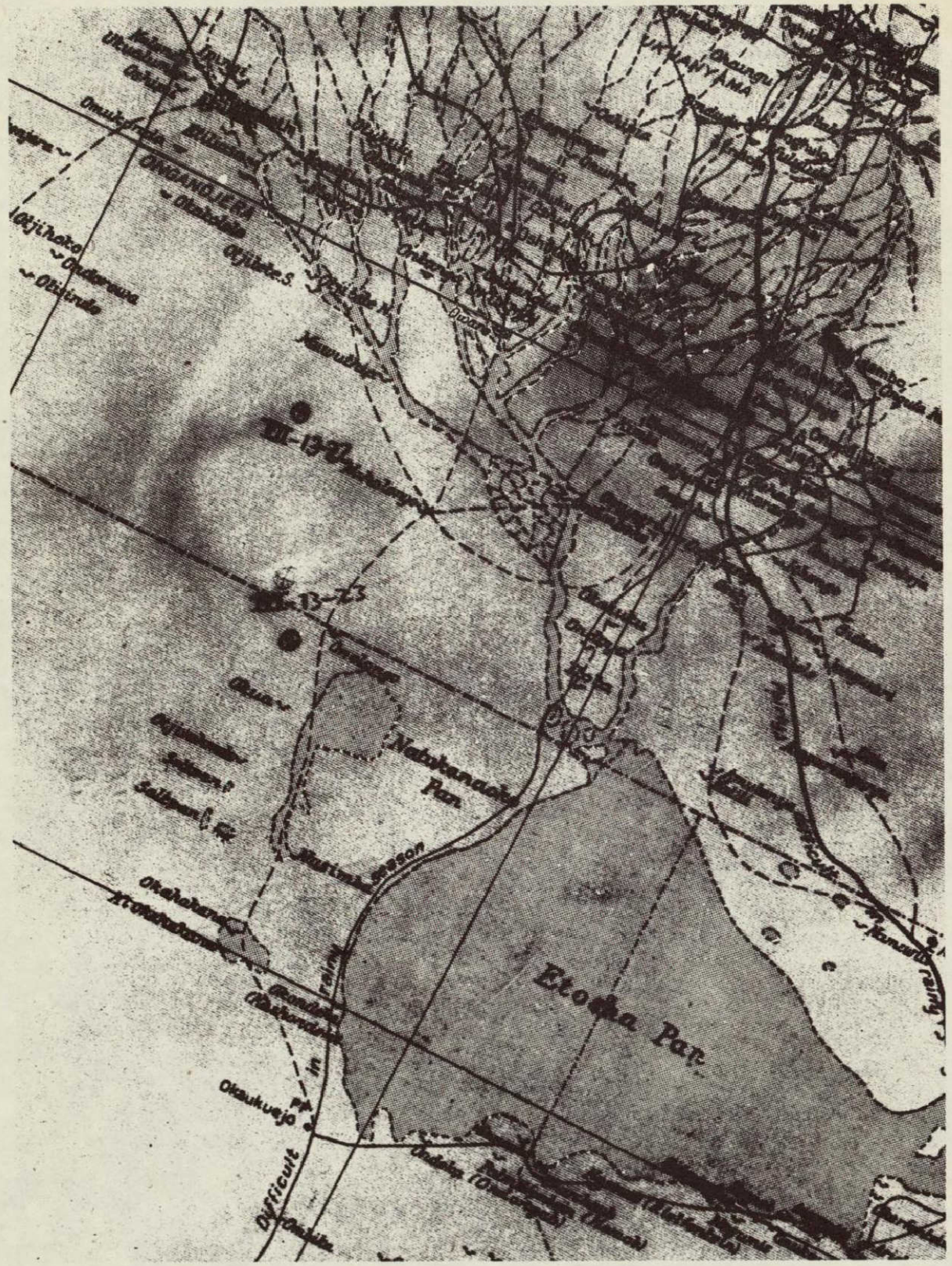

b. AMS SE-33, 1:1,000,000, Enlarged Portion

Figure 16. Gemini V photograph S-65-45733, of Southeast Luzon, Philippine Islands. Indicated are Caramoan Peninsula (A), Lagonoy Bay (B), Tabaco Bay (C), Albay Gulf (D). Peninsula on Caramoan and channels connecting the bays (described in text) are shown by arrows. Distance between points C and D represents about 13 statute miles.

a. Gemini V, S-65 - 45733

b. AMS ND-51, 1:1,000,000, Enlarged Portion

Figure 17. Gemini IV photograph S-65 - 34688, of Northern Chihuahua, Mexico. Palomas volcanic field designated by rectangles on photograph and map. Width of Palomas field (west-east dimension) is about 17 statute miles. Photograph is oblique view to south.

a. Gemini IV, S-65 - 34688

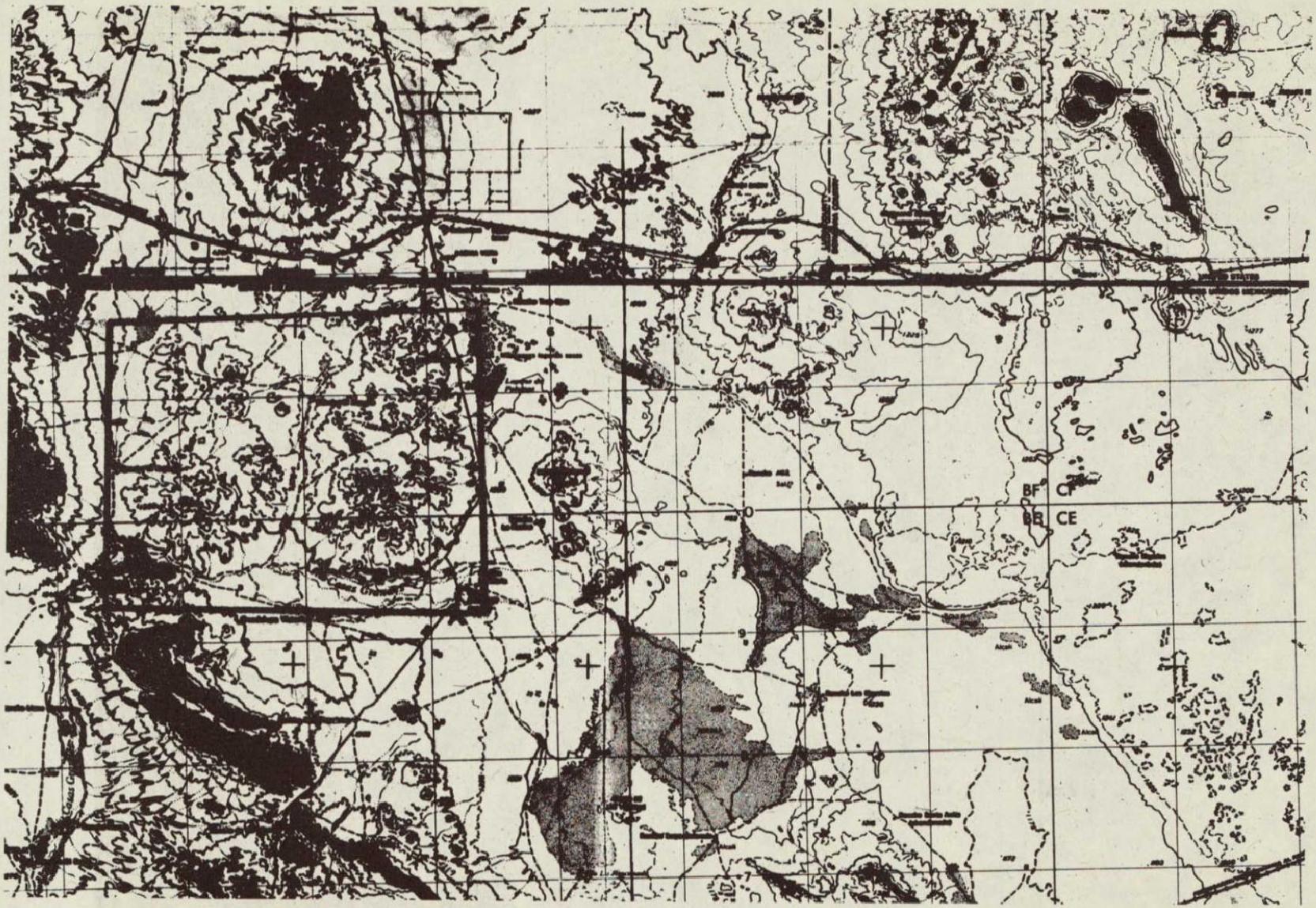

b. AMS El Paso, 1:250,000

Figure 18. Gemini V photograph S-65 - 45793, of Lake Titicaca, Bolivia. Peninsula de Copacabana (A) and Laguna de Uinamarca (B) are indicated. Volcanic plug shown by arrow. Distance between points A and B represents approximately 13 statute miles.

a. Gemini V, S-65 - 45793

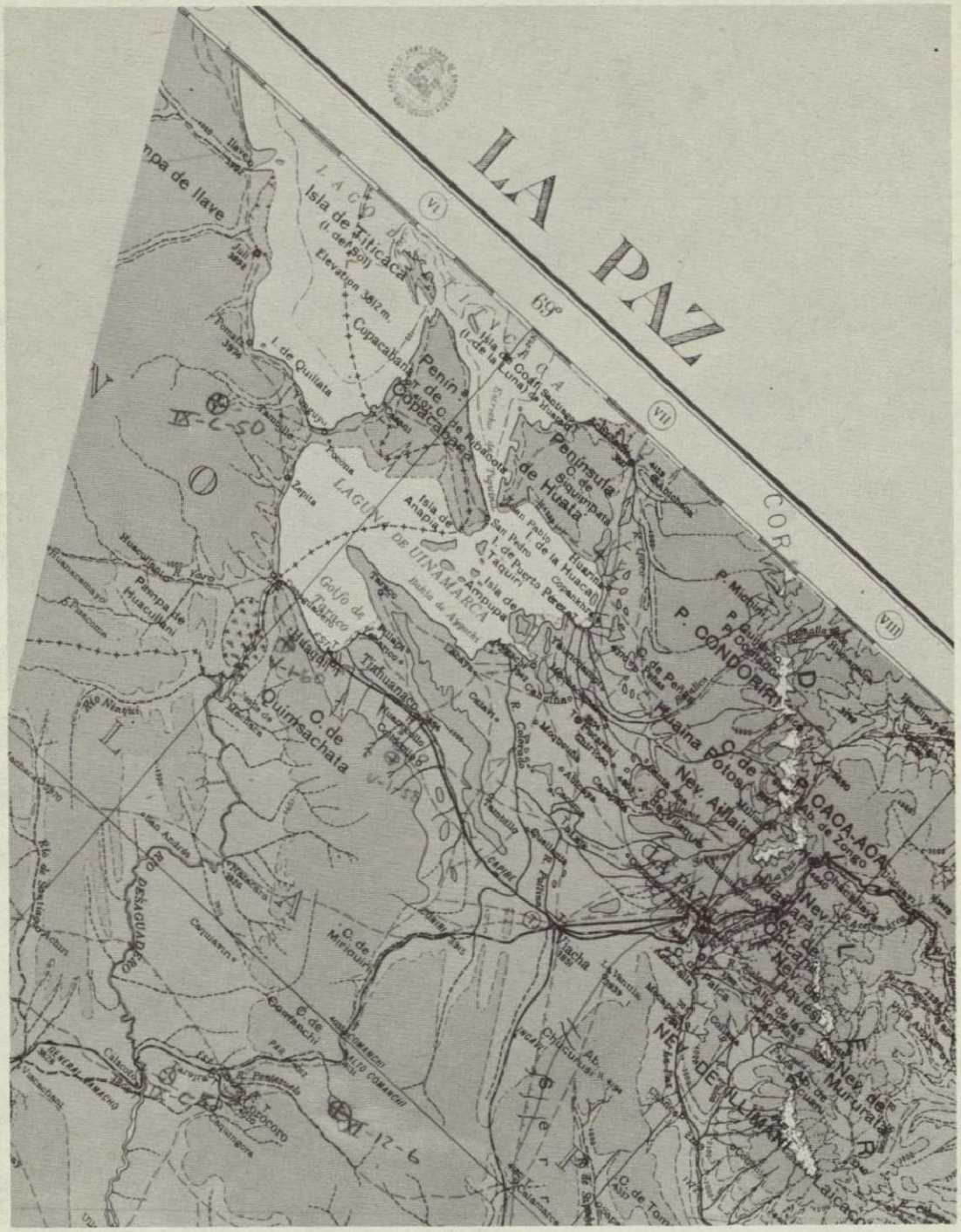

b. AMS SE-19, 1:1,000,000, Enlarged Portion

Figure 19. Gemini XI photographs S-66 - 54528 and S-66 - 54775, of area about northeastern segment of Tibesti Mts., Libya. Indicated are Tibesti Mts., Ergidrisi (arrow tips, on map) and Hamada 1bn Battutah (A). Distance between Tibestis (where labeled) and Hamada 1bn Battutah is about 190 statute miles.

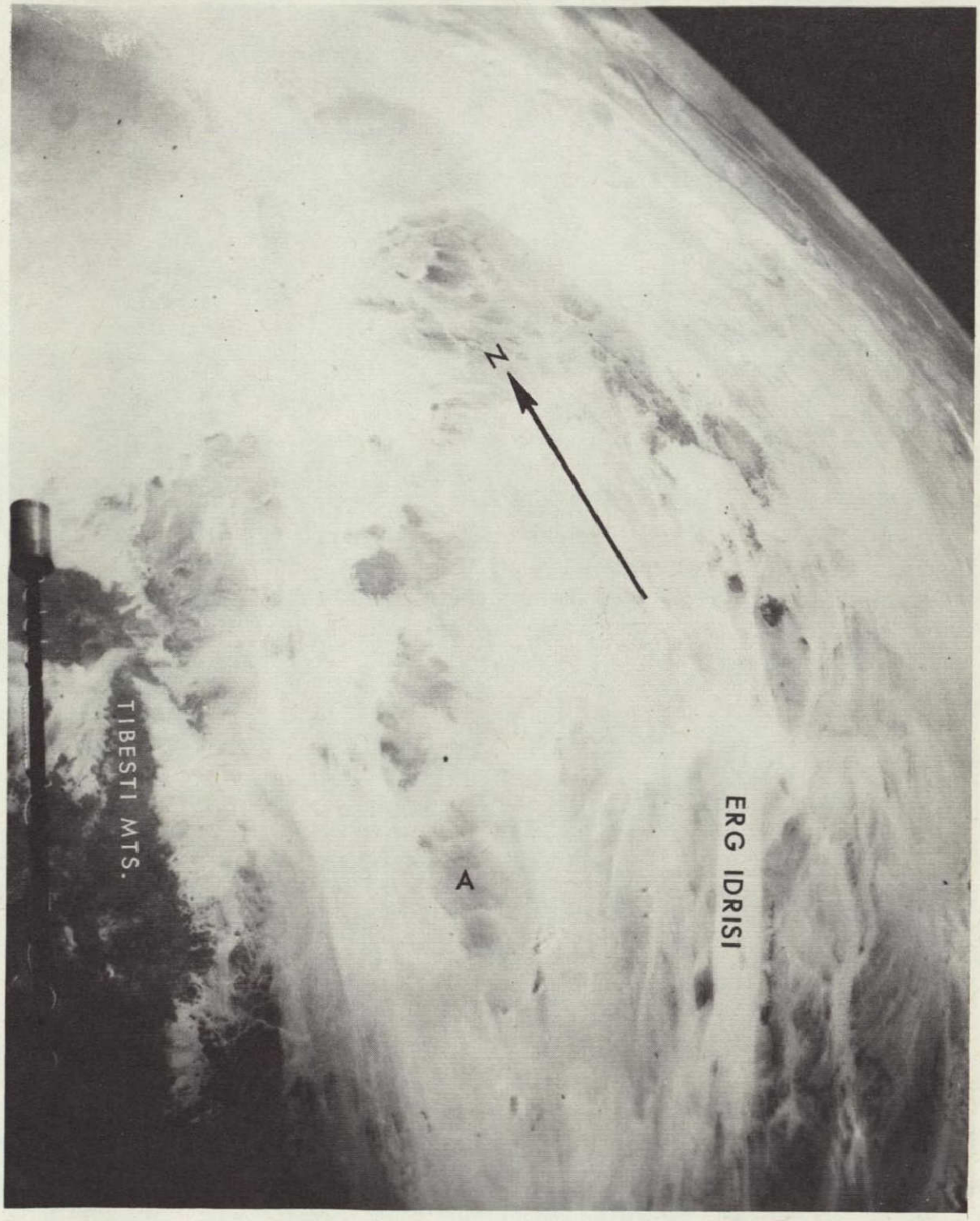

a. Gemini XI, S-66 - 54528

b. Gemini XI, S-66 - 54775

NOT REPRODUCIBLE

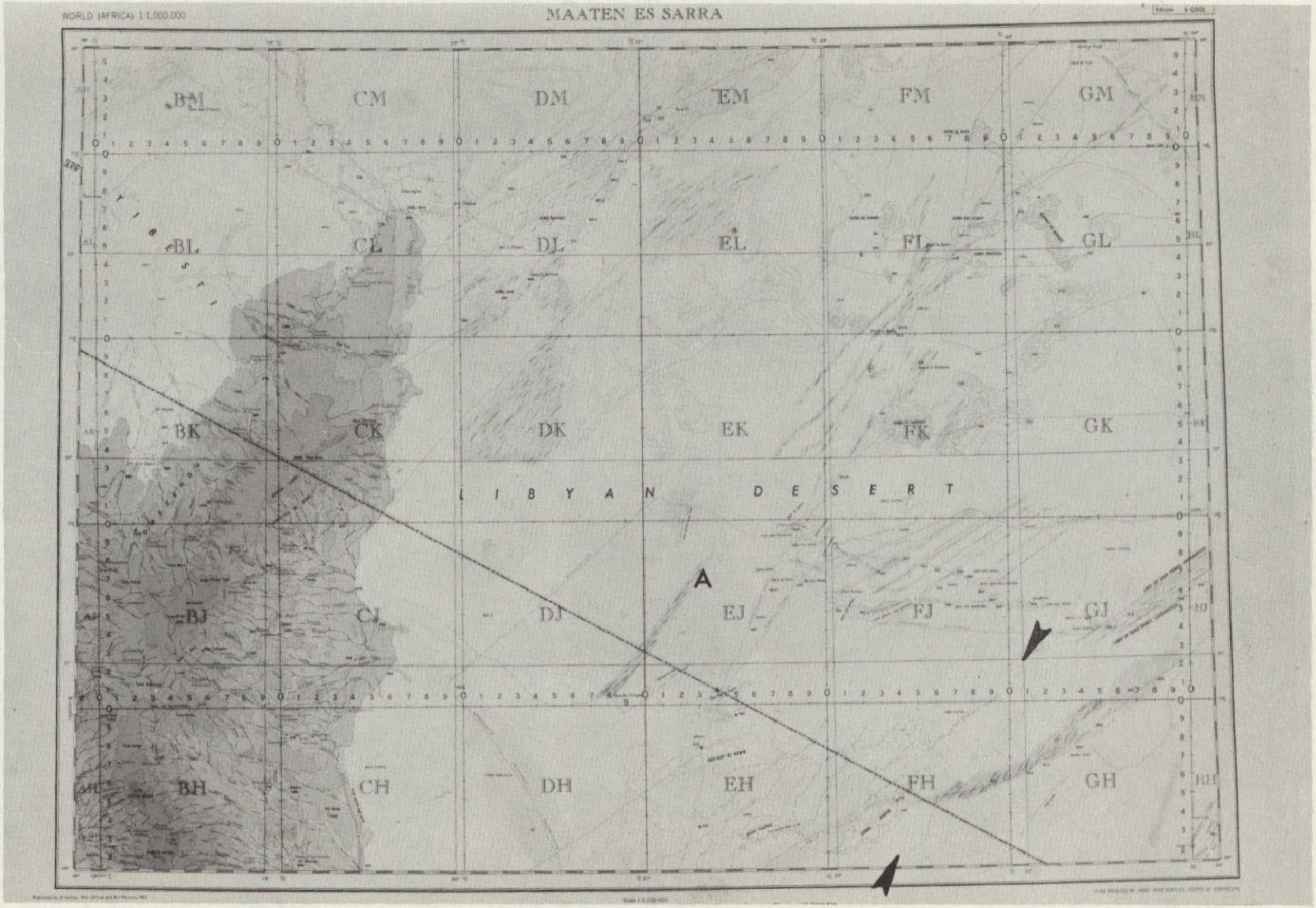

c. AMS NF-34, 1:1,000,000

Figure 20. Low oblique Gemini VI photograph S-65 - 63227, of Comoro Islands. Labeled are Moheli (A), Anjouan (B), and Mayotte (C) Islands. Distance between Anjouan and Mayotte Islands is approximately 38 nautical miles.

a. Gemini VI, S-65 - 63227

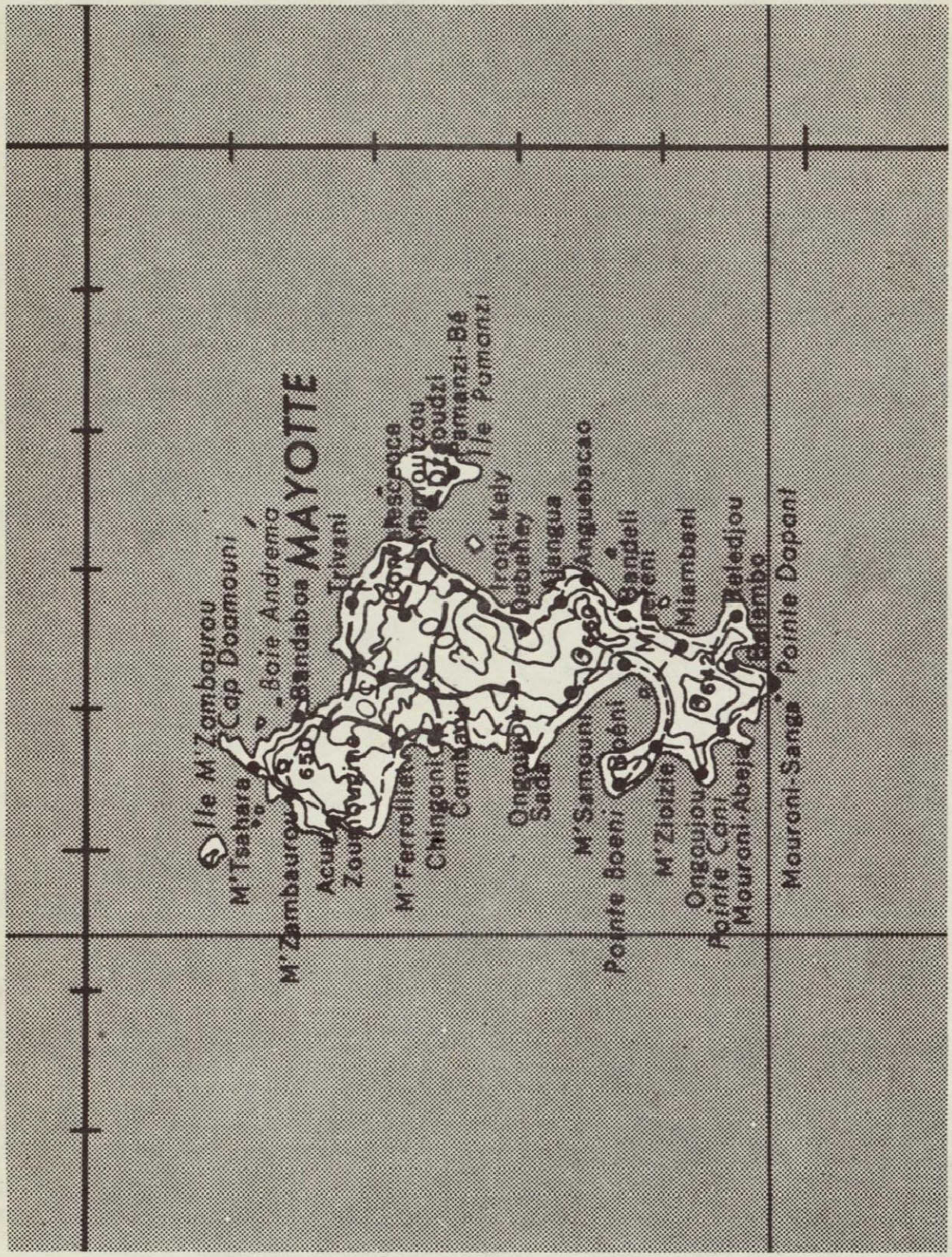

b. AMS SC-38, 1:1,000,000, Enlarged Portion